An introduction to optimal power flow: Theory, formulation, and examples

Stephen Frank & Steffen Rebennack

Taylor & Francis
Taylor & Francis Group

An introduction to optimal power flow: Theory, formulation, and examples

Stephen Frank[a] and Steffen Rebennack[b]

[a]National Renewable Energy Laboratory, Golden, CO, USA; [b]Colorado School of Mines, Golden, CO, USA

ABSTRACT

The set of optimization problems in electric power systems engineering known collectively as Optimal Power Flow (OPF) is one of the most practically important and well-researched subfields of constrained non-linear optimization. OPF has enjoyed a rich history of research, innovation, and publication since its debut five decades ago. Nevertheless, entry into OPF research is a daunting task for the uninitiated—both due to the sheer volume of literature and because OPF's ubiquity within the electric power systems community has led authors to assume a great deal of prior knowledge that readers unfamiliar with electric power systems may not possess. This article provides an introduction to OPF from an operations research perspective; it describes a complete and concise basis of knowledge for beginning OPF research. The discussion is tailored for the operations researcher who has experience with nonlinear optimization but little knowledge of electrical engineering. Topics covered include power systems modeling, the power flow equations, typical OPF formulations, and common OPF extensions.

1. Introduction

The set of optimization problems in electric power systems engineering known collectively as Optimal Power Flow (OPF) is one of the most practically important and well-researched subfields of constrained nonlinear optimization. Carpentier (1962) introduced OPF as an extension to the problem of optimal Economic Dispatch (ED) of generation in electric power systems. Carpentier's key contribution was the inclusion of the electric power flow equations in the ED formulation. Today, the defining feature of OPF remains the presence of the power flow equations in the set of equality constraints.

OPF includes any optimization problem that seeks to optimize the operation of an electric power system subject to the physical constraints imposed by electrical laws and engineering limits. This general framework encompasses dozens of optimization problems for power systems planning and operation (Zhu, 2009; Zhang, 2010; Frank et al., 2012a). As illustrated in Fig. 1, the optimization of power system operation typically occurs via incremental planning: long-term planning procedures make high-level decisions based on coarse system models, whereas short-term procedures refine earlier decisions using detailed models but more limited decision spaces. OPF may be applied to decision-making at nearly any planning horizon—from long-term transmission network capacity planning to minute-by-minute adjustment of real and reactive power dispatch (Wood and Wollenberg, 1996; Glover et al., 2008; Zhu, 2009).

To date, thousands of articles and hundreds of textbook entries have been written about OPF. In its maturation over the past five decades, OPF has served as a practical proving ground for many popular nonlinear optimization algorithms, including gradient methods (Dommel and Tinney, 1968;

Peschon et al., 1972; Alsac and Stott, 1974), Newton-type methods (Sun et al., 1984), sequential linear programming (Stott and Hobson, 1978; Alsac et al., 1990), sequential quadratic programming (Burchett et al., 1982), both linear and nonlinear interior point methods (Vargas et al., 1993; Granville, 1994; Torres and Quintana, 1998), and semi-definite programming (Lavaei and Low, 2012; Low, 2013). These algorithmic approaches, among others, are reviewed in several surveys (Huneault and Galiana, 1991; Momoh et al., 1999a, 1999b; Zhang et al., 2007; Zhang, 2010; Bienstock, 2013), including one recently published by the authors Frank et al. (2012a, 2012b).

Although OPF spans operations research and electrical engineering, the accessibility of the OPF literature skews heavily toward the electrical engineering community. OPF has become sufficiently familiar within the electric power systems community that the recent literature, including survey papers, assumes a great deal of prior knowledge on the part of the reader. Few papers even include a full OPF formulation, much less explain the particulars of the objective function or constraints. Even introductory textbooks (Wood and Wollenberg, 1996; Rau, 2003b; Zhu, 2009) require a strong background in power systems analysis, specifically regarding the form, construction, and solution of the electric power flow equations. Although many electrical engineers have this prior knowledge, an operations researcher likely will not. We believe that this accessibility gap has been detrimental to the involvement of the operations research community in OPF research; our impression is that most OPF articles continue to be published in engineering journals by electrical engineers.

What is missing in the literature—and what we provide in this introductory article—is a detailed introduction to the OPF problem from an operations research perspective.
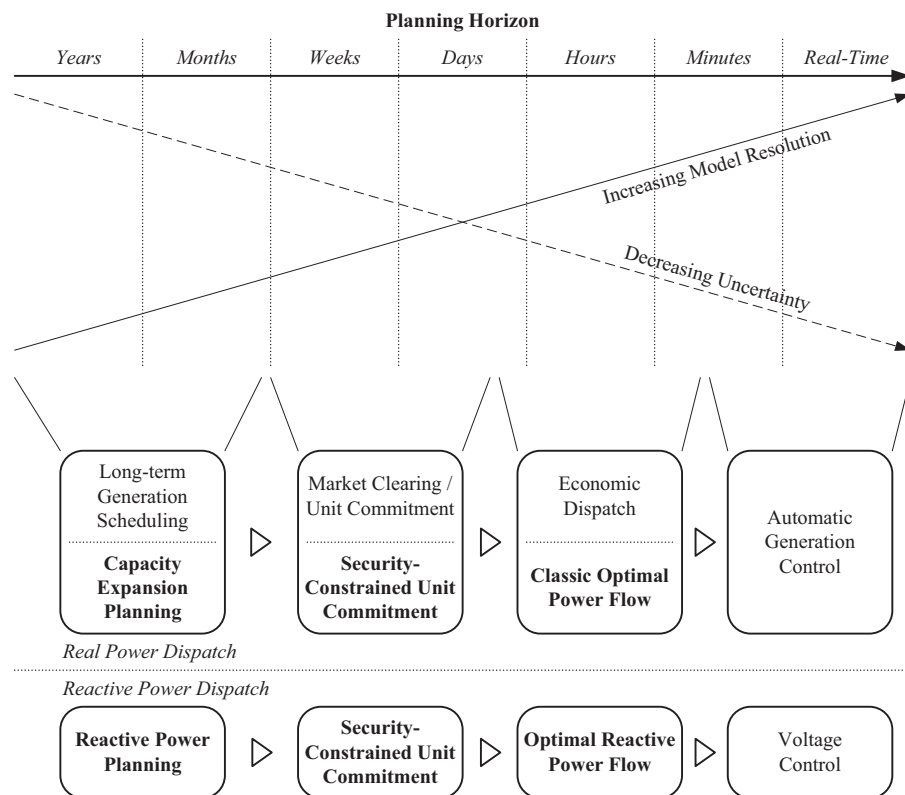
Planning Horizon

Figure 1. Optimization and control procedures for incremental planning of power system operation. Bold text indicates procedures that incorporate variants of optimal power flow.

Existing review articles and surveys (Zhang and Tolbert, 2005; Zhang *et al.*, 2007; Bienstock, 2013), including the authors' recent survey Frank *et al.* (2012a, 2012b), focus heavily on optimization theory and tailored OPF solution algorithms. In contrast, this article emphasizes the electrical engineering theory and mechanics of the OPF formulation. The goal of this article is to provide a bridge between OPF theory and practice: in it we outline the tool set required to understand, formulate, analyze, and ultimately solve a typical OPF problem. Therefore, we address many topics given little attention in other introductory materials, including the construction of the admittance matrix for electrical power flow, treatment of advanced controls such as phase-shifting and tap-changing transformers, a qualitative comparison of the various forms of the electric power flow equations, and various practical considerations, such as the use of the per unit system.

As we have written this article for the operations researcher, we assume that the reader has significant experience with nonlinear optimization and advanced mathematical concepts but little background in electrical engineering. Specifically, this article requires a foundational understanding of

- linear algebra (Greenberg, 1998);
- complex number theory (Greenberg, 1998; Freitag and Busam, 2009);
- analysis of differential equations in the frequency domain (Greenberg, 1998); and
- linear and nonlinear optimization theory and application (Rardin, 1997; Nocedal and Wright, 2006).

We expect that readers may not possess a working knowledge of electrical circuit theory; we therefore provide a brief introduction in Appendix B and recommend O'Malley (2011) for further reading. Readers interested in the technical details of electric power flow should also consult a good power systems text such as Glover *et al.* (2008) or Wood and Wollenberg (1996).

We begin in Section 2 with a description of power systems models, including the classic formulation of the OPF problem. Section 3 surveys some common applications of OPF and includes full formulations for several of the decision processes shown in Fig. 1. Section 4 describes the bus admittance matrix, which is the foundation of the power flow equations. Section 5 reviews the various forms of the power flow equations, with an emphasis on describing their relative advantages and disadvantages. Building on the power flow equations, Section 6 introduces OPF solution methods and practical considerations. Section 7 then provides a worked example of a classic OPF formulation. Finally, Section 8 concludes the article.

We also include four Appendices that provide supplemental information regarding electric power systems modeling and analysis. Appendix A documents the notation used throughout the article, Appendix B reviews fundamental electric power system concepts relevant to OPF, Appendix C summarizes the per-unit system, and Appendix D describes common formats for the exchange of power system data.

Different readers may have different goals in reviewing this article. We recommend that all readers start with the Introduction and Section 2. Readers interested only in a brief OPF overview can subsequently read Sections 3 and 6.2 and safely skip the detailed derivations in other sections. Conversely, readers attempting to implement or test an OPF solution algorithm should read Sections 4 to 7 in detail. Readers interested

primarily in understanding linear approximations for the OPF problem should review Section 5 and in particular Section 5.3, which discusses DC power flow.

2. Modeling of power systems

In this section, we introduce the classic network model for an electric power system and describe conventional power flow and OPF. The development requires some basic knowledge of electrical circuit theory, the frequency domain (phasor) representation of electrical quantities, and the concept of complex electric power. Readers unfamiliar with these topics should consult Appendix B first for a brief overview.

2.1. Notation

Throughout this article, italic roman font (A) indicates a variable or parameter, bold roman font ($\mathbf{A}$) indicates a set, and a tilde over a symbol ($\widetilde{a}$) indicates a phasor quantity (complex number). Letter case does not differentiate variables from parameters; a given quantity may be a variable in some cases and a parameter in others. Symbolic superscripts are used as qualifiers to differentiate similar variables, whereas numeric superscripts indicate mathematical operations. For example, the superscript ^{L} differentiates load power P^L from net power P, but P^2 indicates (net) power squared. Where applicable, electrical units are specified using regular roman font. The unit for a quantity follows the numeric quantity and is separated by a space; for example, 120 V indicates 120 Volts.

We use the following general notation for optimization formulations:

u vector of control variables (independent decision variables);

x vector or state variables (dependent decision variables);

$f(u, x)$ objective function (scalar);

$g(u, x)$ vector function of equality constraints;

$h(u, x)$ vector function of inequality constraints.

In order to remain consistent with the existing body of OPF literature, this article uses notation that follows electrical engineering conventions rather than those of the operations research community. In particular, the symbols e and j represent mathematical constants:

e Euler's number (the base of the natural logarithm), $e \approx 2.71828$; and

j the imaginary unit or 90° operator, $j = \sqrt{-1}$.

This differs from the use of e as the unit vector and j as an index as is common in operations research literature. Appendix A includes a full listing of the notation used in this article, including relevant commentary on other notational differences and a listing of electrical engineering units used in power systems analysis.

2.2. Network representation

Electric power systems may be modeled as a network of electrical buses (nodes) interconnected by branches (arcs or edges) that represent transmission lines, cables, transformers, and similar power systems equipment. Buses represent physical points of interconnection among power systems equipment, whereas branches represent paths for the flow of electrical current. The purpose of an electric power system is to transfer electrical energy from generation (supply) buses to load (demand) buses elsewhere in the network.

Buses are referenced by node with index $i \in \mathbf{N}$, whereas branches are referenced as arcs between nodes $(i, k) \in \mathbf{L}$, where $i, k \in \mathbf{N}$. The undirected graph $(\mathbf{N}, \mathbf{L})$ therefore describes the connectivity of the electrical network. The number of buses and branches are $N = |\mathbf{N}|$ and $L = |\mathbf{L}|$, respectively.

Each system bus i has an associated voltage $\widetilde{V}_i$, which is measured with respect to the system reference (typically Earth ground). When connected via the branch network, or "grid," these voltages induce current in each branch in proportion to the branch admittance. (Admittance, which is a measure of how easily a conductor permits the flow of electrical current, is described in Appendix B.) The most common and concise mathematical description of this phenomenon is the matrix equation

$$\widetilde{I} = \widetilde{Y}\widetilde{V}, \tag{1}$$

in which $\widetilde{V} = (\widetilde{V}_1, \ldots, \widetilde{V}_N)$ is an N-dimensional vector of phasor voltages at each system bus, $\widetilde{I} = (\widetilde{I}_1, \ldots, \widetilde{I}_N)$ is an N-dimensional vector of phasor currents injected into the network at each system bus, and

$$\widetilde{Y} = \begin{pmatrix} \widetilde{Y}_{11} & \cdots & \widetilde{Y}_{1N} \\ \vdots & \ddots & \vdots \\ \widetilde{Y}_{N1} & \cdots & \widetilde{Y}_{NN} \end{pmatrix}$$

is the $N \times N$ complex bus admittance matrix, which is described in detail in Section 4. At each bus i, injection current $\widetilde{I}_i$ represents the net current supplied to the network: generation (supply) minus load (demand). In this framework, voltages $\widetilde{V}$ are state variables that fully characterize system power flow for a given matrix $\widetilde{Y}$.

It is more convenient to work with power flows than currents because (i) injected powers are independent of system voltage angle whereas injected currents are not and (ii) working directly with power allows straightforward computation of required electrical energy via integration with respect to time. Therefore, power systems engineers transform Equation (1) by applying the definition of complex power $S = \widetilde{V}\widetilde{I}^*$ to each side of the matrix equation, as described in Appendix B.4. (Here and elsewhere in this article, the symbol * denotes complex conjugation rather than an optimal value; this use is typical in electrical engineering.) The result is the complex power flow equation

$$S = \widetilde{V} \circ \left(\widetilde{Y}\widetilde{V}\right)^*, \tag{2}$$

in which $S = P + jQ$ is a vector of complex power injections at each bus and $\circ$ denotes element-wise vector multiplication. At each bus i, the total injected power is the difference between the generation S_i^G and the load S_i^L

$$S_i = S_i^G - S_i^L \quad \Leftrightarrow \quad P_i + jQ_i = \left(P_i^G - P_i^L\right) + j\left(Q_i^G - Q_i^L\right).$$

For numerical analysis or optimization, Equation (2) may be decomposed into a set of equivalent, real-valued, nonlinear power flow equations by separating its real and imaginary components (see Section 5).

2.3. Conventional power flow

The conventional Power Flow (PF) problem seeks a deterministic solution to network Equation (2) using numerical analysis techniques. Conventional PF is a feasibility problem: there is no objective function. Rather, the goal is to compute all system bus voltages and power injections. Here, we summarize the PF problem with polar voltage coordinates, which is the classic representation.

If each bus voltage is represented in polar form with magnitude V and phase angle δ, then Equation (2) decomposes into the set of power flow equations

$$P_i(V, \delta) = P_i^{\text{G}} - P_i^{\text{L}} \quad \forall i \in \mathbf{N}, \tag{3}$$

$$Q_i(V, \delta) = Q_i^{\text{G}} - Q_i^{\text{L}} \quad \forall i \in \mathbf{N}, \tag{4}$$

in which net real and reactive power injections P_i and Q_i are trigonometric functions of the system voltages. (See Section 5 for the fully expanded equations.) Each system bus has four variables (net real power injection P_i, net reactive power injection Q_i, voltage magnitude V_i, and voltage angle δ_i) and is governed by two equations. Thus, a deterministic solution to the conventional PF problem requires fixing the values of two out of four variables at each bus.

In conventional PF, all system buses are assigned to one of three bus types.

Slack Bus: At the slack bus, or swing bus, the voltage magnitude and angle are fixed and the power injections are free. The purpose of the slack bus is twofold. First, it provides a voltage reference (typically $V = 1.0$ p.u. and $\delta = 0°$) such that the remaining bus voltages are uniquely determined; we explain the per unit system "p.u." in Appendix C. Second, as it is the only bus at which real power is free to vary, the slack bus is required to ensure that the power flow equations have a feasible solution. There is only one slack bus in a power system model.

Load Bus: At a load bus, or "PQ" bus, the power injections are fixed while the voltage magnitude and angle are free. There are a fixed number of PQ buses in the system; the symbol M denotes this number.

Voltage-Controlled Bus: At a voltage-controlled bus, or "PV" bus, the real power injection and voltage magnitude are fixed while the reactive power injection and the voltage angle are free. (This corresponds to allowing a local source of reactive power to regulate the voltage to a desired setpoint.) There are $N - M - 1$ PV buses in the system.

Assigning buses in this way establishes an equal number of equations and unknowns. Table 1 summarizes the known and unknown quantities for each of the bus types.

Once all voltage magnitudes and angles in the system have been computed, the remaining power injections are trivial to

evaluate via Equations (3) and (4). Solving the PF therefore requires determining $N - 1$ voltage angles (corresponding to the PQ and PV buses) and M voltage magnitudes (corresponding to the PQ buses only). This is done by solving $N + M - 1$ simultaneous nonlinear equations with known right-hand side values. This equation set consists of the real power injection Equation (3) at each PQ and PV bus and the reactive power injection Equation (4) at each PQ bus. Section 6.1 discusses solution methods for these equations.

Even though the power flow equations are nonlinear, there exists only one physically meaningful solution for most power systems models given an equal number of equations and unknowns. Although other mathematically valid solutions sometimes exist, they have no realistic physical interpretation. (An example would be any solution that returns a negative voltage magnitude, as magnitudes are by definition non-negative.) Hence, in practice, conventional PF is an exactly determined problem.

2.4. OPF

OPF combines an objective function with the PF Equations (3) and (4) to form an optimization problem. The presence of the PF equations is the feature that distinguishes OPF from other classes of power systems problems, such as classic ED, Unit Commitment (UC), and market-clearing problems.

Most OPF variants build upon the classic formulation of Carpenter (1962) and Dommel and Tinney (1968). The classic formulation is an extension of classic ED: its objective is to minimize the total cost of electricity generation while maintaining the electric power system within safe operating limits. The power system is modeled as a set of buses $\mathbf{N}$ connected by a set of branches $\mathbf{L}$, with controllable generators located at a subset $\mathbf{G} \subseteq \mathbf{N}$ of the system buses. The operating cost of each generator is a (typically quadratic) function of its real output power: $C_i(P_i^{\text{G}})$. The objective is to minimize the total cost of generation.

The classic form of the formulation is

$$\min \quad \sum_{i \in \mathbf{G}} C_i\left(P_i^{\text{G}}\right), \tag{5}$$

$$\text{s.t.} \quad P_i(V, \delta) = P_i^{\text{G}} - P_i^{\text{L}} \quad \forall i \in \mathbf{N}, \tag{6}$$

$$Q_i(V, \delta) = Q_i^{\text{G}} - Q_i^{\text{L}} \quad \forall i \in \mathbf{N}, \tag{7}$$

$$P_i^{\text{G,min}} \leq P_i^{\text{G}} \leq P_i^{\text{G,max}} \quad \forall i \in \mathbf{G}, \tag{8}$$

$$Q_i^{\text{G,min}} \leq Q_i^{\text{G}} \leq Q_i^{\text{G,max}} \quad \forall i \in \mathbf{G}, \tag{9}$$

$$V_i^{\min} \leq V_i \leq V_i^{\max} \quad \forall i \in \mathbf{N}, \tag{10}$$

$$\delta_i^{\min} \leq \delta_i \leq \delta_i^{\max} \quad \forall i \in \mathbf{N}. \tag{11}$$

Constraints (6) and (7) are the PF equations in polar form. The remaining constraints represent bounds on the system voltages and powers. Typically, load real and reactive power are fixed while generator real and reactive power are control variables subject to minimum and maximum limits. The voltage magnitude and angle at the system slack bus (by convention, bus 1) are also fixed, usually to $\tilde{V}_1 = 1.0\angle 0$.

Table 1. Power system bus types and characteristics for conventional power flow.

Bus type	Slack	PQ	PV
Number of buses in system	1	M	$N - M - 1$
Known quantities	δ, V	P, Q	P, V
Unknown quantities	P, Q	δ, V	δ, Q
Number of equations in conventional PF	0	2	1

Early methods partition the decision variables into a set of control variables u (typically the controllable bus power injections) and a set of state variables x (the voltage magnitudes and angles; Dommel and Tinney, 1968; Burchett *et al*, 1982). Under this framework, the vector of control variables (independent decision variables) for the classic formulation is

$$u = \left(P^{\mathrm{G}}_{i:i\in\mathbf{G}}, Q^{\mathrm{G}}_{i:i\in\mathbf{G}} \right)$$

and the vector of state variables (dependent decision variables) is

$$x = \left(\delta_2, \dots, \delta_N, V_2, \dots, V_N \right).$$

Although not considered in the earliest papers, more recent OPF formulations may include branch current limits and, if applicable, box constraints related to the operational limits of PF control devices. These and other side constraints are discussed in Section 5.5.

2.5. Challenges

Power systems have evolved significantly since the early days of OPF, in particular through the addition of advanced controls. Modern grids include control devices that are difficult to incorporate into OPF formulations: on-load tap changers (Acha *et al*., 2000), phase shifters (Momoh *et al*., 2001), series and shunt capacitors (Momoh *et al*., 1997), and flexible AC transmission systems devices (Xiao *et al*., 2002). As such controls exert a large influence on system power flows, they cannot be neglected in practical OPF formulations. Unfortunately, many academic papers neglect the modeling of advanced controls and treat only the classic formulation, limiting their application in a practical setting.

Nevertheless, some researchers have dedicated considerable effort to developing accurate but efficient models for advanced controls (Acha *et al*., 2000; Lehmköster, 2002; Xiao *et al*., 2002). Most such models employ auxiliary power injections at certain system buses coupled with side constraints to enforce power balance. However, even a modest number of such constraints can significantly increase OPF problem complexity (Azevedo *et al*., 2010). Many devices also have discrete control settings, which if accurately modeled create a large and intractable Mixed-Integer Nonlinear Programming (MINLP) problem (Soler *et al*., 2012). A typical approach is to model the control space as continuous and round the optimal solution to the nearest discrete value (Adibi *et al*., 2003), but this heuristic can yield suboptimal or infeasible solutions (Capitanescu and Wehenkel, 2010; Soler *et al*., 2012).

Even without variable phase angles, variable tap ratios, or branch current limits, the classic OPF formulation is difficult to solve. The power flow constraints (6) and (7) are both nonlinear and non-convex, and the presence of trigonometric functions complicates the construction of approximations. Moreover, because OPF is tightly constrained, local optima often provide only incremental improvements with respect to the system starting point. Thus, the optimum may only improve a few percent upon the base case, as illustrated by numerical results in

Alsac and Stott (1974), Sun *et al*. (1984), Granville (1994), and many other papers.

For these reasons, OPF problems have historically been solved using tailored algorithms rather than general-purpose solvers. Although effective for research problems, few such algorithms are considered sufficiently reliable for industrial deployment. In particular, solution methods for both conventional PF and OPF become significantly less reliable when the power system is under stress (Bienstock, 2013). Algorithm robustness is also a key concern: small changes in the power system state may lead to the loss of local feasibility (a critical issue for local nonlinear solvers) or large changes in the optimal solution (Almeida and Galiana, 1996). In addition, real power system models include thousands of buses; problems of this size present computational challenges for state-of-the-art nonlinear solvers.

In actual practice, almost all practical OPF problems are solved using a linear (DC) power flow approximation (Section 5.3; Rau, 2003a; Stott *et al*., 2009). The results of the DC-OPF are then used either for contingency analysis with conventional AC-PF or, less commonly, to initialize, or "warm start," a nonlinear OPF (AC-OPF). Unfortunately, the DC formulation can exhibit significant inaccuracy, particularly for heavily loaded transmission lines (Momoh *et al*., 1997; Stott *et al*., 2009). Nor is the DC model applicable to reactive power dispatch. The search for reliable AC-OPF solution methods therefore remains extremely relevant to the power systems community.

3. Applications of OPF

In addition to the classic ED formulation, several other OPF variants are common in both industry and research. These include Security-Constrained Economic Dispatch (SCED), Security-Constrained Unit Commitment (SCUC), Optimal Reactive Power Flow (ORPF), and Reactive Power Planning (RPP).

3.1. Security-Constrained Economic Dispatch

SCED, sometimes referred to as security-constrained optimal power flow, is an OPF formulation that includes power system contingency constraints (Alsac and Stott, 1974). A contingency is defined as an event that removes one or more generators or transmission lines from the power system, increasing the stress on the remaining network. SCED seeks an optimal solution that remains feasible under any of a pre-specified set of likely contingency events. SCED is a restriction of the classic OPF formulation: for the same objective function, the optimal solution to SCED will be no better than the optimal solution without considering contingencies. The justification for the restriction is that SCED mitigates the risk of a system failure (blackout) should one of the contingencies occur.

SCED formulations typically have the same objective function and decision variables u as the classic formulation, except that the slack bus real and reactive power are considered state variables, as they must be allowed to change in order for the system to remain feasible during each contingency. However, SCED introduces N_C additional sets of state variables x and accompanying sets of power flow constraints, where N_C is the number of

contingencies. SCED can be expressed in a general way as

$$
\begin{aligned}
\min \quad & f(u, x_0), \\
\text{s.t.} \quad & g_0(u, x_0) = 0, \\
& h_0(u, x_0) \leq 0, \\
& g_c(u, x_c) = 0 \quad \forall\, c \in \mathbf{C}, \\
& h_c(u, x_c) \leq 0 \quad \forall\, c \in \mathbf{C}, \qquad (12)
\end{aligned}
$$

where $\mathbf{C} = \{1, \ldots, N_C\}$ is the set of contingencies to consider. Each contingency has a distinct admittance matrix $\widetilde{Y}_c$, typically with less connectivity than the original system. Apart from the contingency index, f, g, and h are defined as the objective function, equality constraints, and inequality constraints in the classic OPF formulation (5) to (11), respectively.

For each contingency $c \in \mathbf{C}$, the post-contingency power flow must remain feasible for the original decision variables u:

(i) the power flow equations must have a solution;
(ii) the contingency state variables x_c must remain within limits; and
(iii) any inequality constraints, such as branch flow limits, must be satisfied.

One very common contingency set considers independently the loss of each generator and each non-radial transmission line. The resulting SCED solution is said to be $N - 1$ reliable, since for every possible single element contingency c the network has a feasible solution x_c given the optimal dispatch decisions u.

Typically, the limits on the contingency-dependent state variables x_c and other functional inequality constraints are relaxed for the contingency cases compared to the base case. For example, system voltages are allowed to dip further during an emergency than under normal operating conditions. The relaxation of system limits is justified because operation under a contingency is temporary: when a contingency occurs, operators immediately begin re-configuring the system to return all branches and buses to normal operating limits. For the same reason, the SCED objective function considers only the base case: contingency cases are improbable and transient and do not contribute to the expected cost function.

SCED has interesting connections to other areas of optimization. The motivation for SCED is theoretically similar to that of Robust Optimization (RO) (Bertsimas *et al.*, 2011), although RO typically addresses continuous uncertain parameters rather than discrete scenarios. Additionally, because the constraints are separable for a fixed u, SCED lends itself well to parallelization and decomposition algorithms (Qiu *et al.*, 2005).

3.2. Security-Constrained Unit Commitment

In electric power systems operation, unit commitment (UC) refers to the scheduling of generating units such that total operating cost is minimized. UC differs from ED in that it operates across multiple time periods and schedules the on–off status of each generator in addition to its power output. UC must address generator startup and shutdown time and costs, limits on generator cycling, ramp rate limits, reserve margin requirements, and other scheduling constraints. UC is a large-scale, multi-period MINLP. Many UC formulations relax certain aspects of

the problem in order to obtain a mixed-integer linear program instead—for instance, by using linearized cost functions.

If the power flow equations are added to the UC problem, the formulation becomes SCUC. In SCUC, a power flow is applied at each time period to ensure that the scheduled generation satisfies not only the scheduling constraints but also system voltage and branch flow limits. In other words, SCUC ensures that the UC algorithm produces a generation schedule that can be physically realized in the power system. Due to its complexity, research on SCUC has accelerated only with the advent of faster computing capabilities and algorithmic advancements.

In SCUC, we introduce a time index $t \in \mathbf{T}$ and a set of binary control variables w_{it} to the OPF formulation. Each w_{it} indicates whether or not generator i is committed for time period t. The modified formulation becomes

$$
\min \quad \sum_{t \in \mathbf{T}} \sum_{i \in \mathbf{G}} \Big(w_{it} C_i \big(P_{it}^{\mathrm{G}}\big) + C_i^{\mathrm{SU}} w_{it} \big(1 - w_{i,t-1}\big)
$$
$$
+ C_i^{\mathrm{SD}} \big(1 - w_{it}\big) w_{i,t-1} \Big), \qquad (13)
$$

$$
\text{s.t.} \quad P_{it}\left(V_t, \delta_t, \varphi_t, T_t\right) = P_{it}^{\mathrm{G}} - P_{it}^{\mathrm{L}} \quad \forall\, i \in \mathbf{N}, \forall\, t \in \mathbf{T}, \tag{14}
$$

$$
Q_{it}\left(V_t, \delta_t, \varphi_t, T_t\right) = Q_{it}^{\mathrm{G}} - Q_{it}^{\mathrm{L}} \quad \forall\, i \in \mathbf{N}, \forall\, t \in \mathbf{T}, \tag{15}
$$

$$
w_{it} P_i^{\mathrm{G,min}} \leq P_{it}^{\mathrm{G}} \leq w_{it} P_i^{\mathrm{G,max}} \quad \forall\, i \in \mathbf{G}, \forall\, t \in \mathbf{T}, \tag{16}
$$

$$
w_{it} Q_i^{\mathrm{G,min}} \leq Q_{it}^{\mathrm{G}} \leq w_{it} Q_i^{\mathrm{G,max}} \quad \forall\, i \in \mathbf{G}, \forall\, t \in \mathbf{T}, \tag{17}
$$

$$
V_i^{\mathrm{min}} \leq V_{it} \leq V_i^{\mathrm{max}} \quad \forall\, i \in \mathbf{N}, \forall\, t \in \mathbf{T}, \tag{18}
$$

$$
\delta_i^{\mathrm{min}} \leq \delta_{it} \leq \delta_i^{\mathrm{max}} \quad \forall\, i \in \mathbf{N}, \forall\, t \in \mathbf{T}, \tag{19}
$$

$$
\varphi_{ik}^{\mathrm{min}} \leq \varphi_{ikt} \leq \varphi_{ik}^{\mathrm{max}} \quad \forall\, ik \in \mathbf{H}, \forall\, t \in \mathbf{T}, \tag{20}
$$

$$
T_{ik}^{\mathrm{min}} \leq T_{ikt} \leq T_{ik}^{\mathrm{max}} \quad \forall\, ik \in \mathbf{K}, \forall\, t \in \mathbf{T}, \tag{21}
$$

$$
I_{ikt}\left(V_t, \delta_t\right) \leq I_{ik}^{\mathrm{max}} \quad \forall\, ik \in \mathbf{L}, \forall\, t \in \mathbf{T}, \tag{22}
$$

$$
P_i^{\mathrm{Down}} \leq P_{it}^{\mathrm{G}} - P_{i,t-1}^{\mathrm{G}} \leq P_i^{\mathrm{Up}} \quad \forall\, i \in \mathbf{G}, \forall\, t \in \mathbf{T}, \tag{23}
$$

$$
\sum_{i \in \mathbf{G}} w_{it} P_i^{\mathrm{G,max}} - \sum_{i \in \mathbf{G}} P_{it}^{\mathrm{G}} \geq P_{\mathrm{Reserve}} \quad \forall\, t \in \mathbf{T}. \tag{24}
$$

The objective function (13) includes terms for unit startup costs C^{SU} and shutdown costs C^{SD} in addition to the generation costs in each time period. The PF Equations (14) and (15) are generalized to include the effects of phase-shifting and tap-changing transformers (Section 5.5. We abuse notation slightly by using $(V_t, \delta_t, \varphi_t, T_t)$ to represent the vector of all voltage magnitudes, voltage angles, and engineering control settings for time period t.) The generation limits (16) and (17) are modified such that uncommitted units must have zero real and reactive power generation. Box constraints (20) and (21) enforce engineering control limits and (22) limits the current on each transmission line; these constraints and associated sets $\mathbf{H}$ and $\mathbf{K}$ are described in detail in Section 5.5. Constraint (23) specifies positive and negative generator ramp limits P^{Up} and P^{Down}, respectively; these are

physical limitations of the generators. Constraint (24) requires a spinning reserve margin of at least P_{Reserve}; sometimes this constraint is written such that P_{Reserve} is a fraction of the total load in each time period.

The SCUC formulation (13)–(24) is one of many possible formulations. Some formulations include more precise ramp limits and startup and shutdown characteristics; others include constraints governing generator minimum uptime and downtime. Due to of the scale and presence of binary decision variables, SCUC is one of the most difficult power systems optimization problems. Bai and Wei (2009) and Zhu (2009) provide more discussion of SCUC, including detailed formulations.

More broadly, SCUC belongs to a class of problems known as multi-period or dynamic OPF. Dynamic OPF problems span multiple time periods. Mathematically, each time period requires a single copy of the underlying PF equations; the dimensionality therefore scales linearly with the time horizon. Coupling constraints then link the different time periods. In the case of the SCUC, the ramping constraints (23) provide this coupling. Grid-scale storage systems, such as batteries, also require coupling constraints that create dynamic OPF problems (Snyder, 2013). Other examples include system design problems such as discussed in Frank and Rebennack (2015), where multiple OPF problems are coupled by binary design variables.

3.3. Optimal Reactive Power Flow

ORPF, also known as reactive power dispatch or VAR control, seeks to optimize the system reactive power generation in order to minimize the total system losses. In ORPF, the system real power generation is determined *a priori*, from the outcome of, for example, a DC-OPF algorithm, UC, or another form of ED. A basic ORPF formulation is

$$\min \quad P_1, \tag{25}$$

$$\text{s.t.} \quad P_i\left(V, \delta, \varphi, T\right) = P_i^{\text{G}} - P_i^{\text{L}} \quad \forall\, i \in \mathbf{N}, \tag{26}$$

$$Q_i\left(V, \delta, \varphi, T\right) = Q_i^{\text{G}} - Q_i^{\text{L}} \quad \forall\, i \in \mathbf{N}, \tag{27}$$

$$Q_i^{\text{G,min}} \le Q_i^{\text{G}} \le Q_i^{\text{G,max}} \quad \forall\, i \in \mathbf{G}, \tag{28}$$

$$V_i^{\min} \le V_i \le V_i^{\max} \quad \forall\, i \in \mathbf{N}, \tag{29}$$

$$\delta_i^{\min} \le \delta_i \le \delta_i^{\max} \quad \forall\, i \in \mathbf{N}, \tag{30}$$

$$\varphi_{ik}^{\min} \le \varphi_{ik} \le \varphi_{ik}^{\max} \quad \forall\, ik \in \mathbf{H}, \tag{31}$$

$$T_{ik}^{\min} \le T_{ik} \le T_{ik}^{\max} \quad \forall\, ik \in \mathbf{K}, \tag{32}$$

$$I_{ik}\left(V, \delta\right) \le I_{ik}^{\max} \quad \forall\, ik \in \mathbf{L}. \tag{33}$$

The power flow Equations (26) and (27) are again generalized to include the effects of phase-shifting and tap-changing transformers (Section 5.5). The vector of control variables is

$$u = \left(P_1, Q_{i:i\in\mathbf{G}}^{\text{G}}, \varphi_{ik:ik\in\mathbf{H}}, T_{ik:ik\in\mathbf{K}}\right),$$

while the vector of state variables $x = (\delta, V)$ is identical to the classic formulation. In ORPF, all real power load and generation is fixed except for the real power at the slack bus, P_1. Minimizing P_1 is therefore equivalent to minimizing total system loss.

One motivation for using ORPF is the reduction of the variable space compared with fully coupled OPF (Contaxis *et al.*,

1986); another is the ability to reschedule reactive power to optimally respond to changes in the system load without changing previously established real power setpoints. Many interior point algorithms for OPF have focused specifically on ORPF (Frank *et al.*, 2012a). Zhu (2009, Ch. 10) discusses several approximate ORPF formulations and their solution methods.

3.4. Reactive Power Planning

RPP extends the ORPF problem to the optimal allocation of new reactive power sources—such as capacitor banks—within a power system in order to minimize either system losses or total costs. RPP modifies ORPF to include a set of possible new reactive power sources; the presence or absence of each new source is modeled with a binary variable. The combinatorial nature of installing new reactive power sources has inspired many papers that apply heuristic methods to RPP (Frank *et al.*, 2012b).

A basic RPP formulation that minimizes total costs is

$$\min \quad C_1\left(P_1\right) + \sum_{i\in\mathbf{Q}} w_i C_i^{\text{Install}}, \tag{34}$$

$$\text{s.t.} \quad P_i\left(V, \delta, \varphi, T\right) = P_i^{\text{G}} - P_i^{\text{L}} \quad \forall\, i \in \mathbf{N}, \tag{35}$$

$$Q_i\left(V, \delta, \varphi, T\right) = Q_i^{\text{G}} + Q_i^{\text{New}} - Q_i^{\text{L}} \quad \forall\, i \in \mathbf{N}, \tag{36}$$

$$Q_i^{\text{G,min}} \le Q_i^{\text{G}} \le Q_i^{\text{G,max}} \quad \forall\, i \in \mathbf{G}, \tag{37}$$

$$w_i Q_i^{\text{New,min}} \le Q_i^{\text{New}} \le w_i Q_i^{\text{New,max}} \quad \forall\, i \in \mathbf{Q}, \tag{38}$$

$$V_i^{\min} \le V_i \le V_i^{\max} \quad \forall\, i \in \mathbf{N}, \tag{39}$$

$$\delta_i^{\min} \le \delta_i \le \delta_i^{\max} \quad \forall\, i \in \mathbf{N}, \tag{40}$$

$$\varphi_{ik}^{\min} \le \varphi_{ik} \le \varphi_{ik}^{\max} \quad \forall\, ik \in \mathbf{H}, \tag{41}$$

$$T_{ik}^{\min} \le T_{ik} \le T_{ik}^{\max} \quad \forall\, ik \in \mathbf{K}, \tag{42}$$

$$I_{ik}\left(V, \delta\right) \le I_{ik}^{\max} \quad \forall\, ik \in \mathbf{L}, \tag{43}$$

where C_i^{Install} represents the capital cost of each new reactive power source $i \in \mathbf{Q}$; Q_i^{New} is the amount of reactive power provided by each new reactive power source, subject to limits $Q_i^{\text{New,min}}$ and $Q_i^{\text{New,max}}$; and w_i is a binary variable governing the decision to install each new reactive power source. The modified vector of control variables is

$$u = \left(P_1, Q_{i:i\in\mathbf{G}}^{\text{G}}, w_{i:i\in\mathbf{Q}}, Q_{i:i\in\mathbf{Q}}^{\text{New}}, \varphi_{ik:ik\in\mathbf{H}}, T_{ik:ik\in\mathbf{K}}\right).$$

Some variants of RPP also include real power dispatch in the decision variables or include multiple load scenarios.

By necessity, RPP optimizes with respect to uncertain future conditions—typically reactive power requirements for worst-case scenarios. This uncertainty, together with the problem complexity, make RPP a very challenging optimization problem (Zhang *et al.*, 2007). Zhang and Tolbert (2005) review both formulations and solution techniques for RPP.

4. The admittance matrix

The PF equations are the defining constraints in OPF, and the bus admittance matrix $\widetilde{Y}$ in turn forms the core of the PF equations. OPF data sources do not typically provide $\widetilde{Y}$ directly,
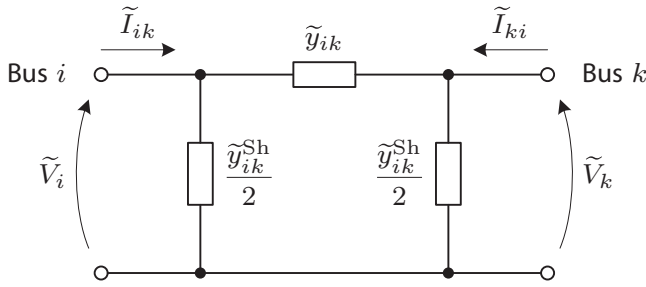
Figure 2. Π branch model.

and we therefore summarize the theory and mechanics of its construction here. Readers uninterested in the electrical engineering details may wish to skip this section; such readers may reference Equations (53) to (56) as needed for the mathematical definition of the matrix elements.

The elements of $\widetilde{Y}$ derive from the application of Ohm's and Kirchoff's laws (Appendix B) to a steady-state AC electrical network. Recall from Section 2.2 that the set of buses $\mathbf{N}$ and set of branches $\mathbf{L}$ form undirected graph $(\mathbf{N}, \mathbf{L})$ that describes the electrical network. Each branch $(i, k) \in \mathbf{L}$ has an associated *series* admittance $\widetilde{y}_{ik}$ that governs the voltage–current relationship between buses i and k. According to Kirchoff's Voltage Law (KVL) and Ohm's law,

$$\widetilde{I}_{ik} = \left(\widetilde{V}_i - \widetilde{V}_k\right)\widetilde{y}_{ik}, \tag{44}$$

in which $\widetilde{I}_{ik}$ is the current flowing through branch ik from bus i to bus k. Branches may also have an associated *shunt* admittance $\widetilde{y}_{ik}^{\mathrm{Sh}}$, which represents leakage of current from within the branch to the reference node. In physical terms, this leakage occurs all along the branch, but in the model the shunt admittance is applied in equal parts to the buses at each end of the branch as illustrated in Fig. 2. This representation is called the Π branch model.

By Kirchoff's Current Law (KCL), the current $\widetilde{I}_i$ injected into bus i must exactly equal the sum of all currents flowing out of bus i via the various series and shunt admittances, including any shunt admittance $\widetilde{y}_i^{\mathrm{S}}$ associated with the bus itself. Neglecting off-nominal branch turns ratios (described in Section 4.1), the bus injection current is

$$\widetilde{I}_i = \widetilde{V}_i \left(\widetilde{y}_i^{\mathrm{S}} + \frac{1}{2} \sum_{k:(i,k)\in\mathbf{L}} \widetilde{y}_{ik}^{\mathrm{Sh}} + \frac{1}{2} \sum_{k:(k,i)\in\mathbf{L}} \widetilde{y}_{ki}^{\mathrm{Sh}} \right)$$
$$+ \sum_{k:(i,k)\in\mathbf{L}} \left(\widetilde{V}_i - \widetilde{V}_k\right)\widetilde{y}_{ik} + \sum_{k:(k,i)\in\mathbf{L}} \left(\widetilde{V}_i - \widetilde{V}_k\right)\widetilde{y}_{ki}. \tag{45}$$

Matrix Equation (1) is equivalent to Equation (45) if the elements of $\widetilde{Y}$ are defined as

$$\widetilde{Y}_{ii} = \text{sum of all admittances connected to bus } i$$
$$-\widetilde{Y}_{ik} = \text{sum of all admittances connected between bus } i \text{ and}$$
$$\text{bus } k \tag{46}$$

Since only a single branch (i, k) connects bus i to bus k, the off-diagonal elements become $\widetilde{Y}_{ik} = \widetilde{Y}_{ki} = -\widetilde{y}_{ik}$. If there is no connection between buses i and k, $\widetilde{Y}_{ik} = 0$. Typically, each bus connects to only a few branches, such that $L \in \mathrm{O}(N)$. Thus, $\widetilde{Y}$

is sparse, having dimension $N \times N$ but only $N + 2L$ non-zero entries.

4.1. Branch models

The Π model of Fig. 2 is sufficient for modeling the majority of power systems branch elements, including transmission lines, cables, and transformers. Most power systems transformers have nominal turns ratios; that is, the voltage ratio across the transformer exactly equals change in system voltage base across the transformer (a 1:1 voltage ratio in per unit, with no phase shift). As the per unit system automatically accounts for nominal turns ratios (see Appendix C), no corrections to the admittance matrix are necessary.

Some transformers, however, do not have exactly a 1:1 voltage ratio in per unit. Such transformers are labeled "off-nominal"; this category includes fixed-tap transformers with other than unity turns ratios, tap-changing transformers, and phase-shifting transformers. In practical power system models, improperly neglecting off-nominal turns ratios may severely distort computed PF, such that any resulting OPF solution may be unusable. Therefore, off-nominal transformers require modified entries in $\widetilde{Y}$ to account for the additional voltage magnitude or phase angle change relative to the nominal case.

The generalized Π branch model in Fig. 3 extends the Π model to accommodate both nominal and off-nominal turns ratios. The model includes series admittance $\widetilde{y}_{ik}$, shunt admittance $\widetilde{y}_{ik}^{\mathrm{Sh}}$, and an ideal transformer. Bus i is the *tap bus* and bus k is the *impedance bus*, or *Z bus*. The transformer turns ratio in per unit is $a:1$, where a is a complex exponential consisting of magnitude T and phase shift φ

$$a = Te^{j\varphi},$$

such that in the figure $\widetilde{V}_i = a\widetilde{V}_i'$ and $\widetilde{I} = \widetilde{I}_{ik}'/a^*$. (To simplify the mathematical presentation, we abuse notation throughout this section by omitting the subscript ik on a, T, and φ.) Selecting $T = 1$ and $\varphi = 0$ yields the nominal turns ratio.

In order to model the effects of the off-nominal turns ratio, we require a partial admittance matrix $\widetilde{Y}'$ such that

$$\begin{pmatrix} \widetilde{I}_{ik} \\ \widetilde{I}_{ki} \end{pmatrix} = \begin{pmatrix} \widetilde{Y}_{ii}' & \widetilde{Y}_{ik}' \\ \widetilde{Y}_{ki}' & \widetilde{Y}_{kk}' \end{pmatrix} \begin{pmatrix} \widetilde{V}_i \\ \widetilde{V}_k \end{pmatrix}.$$

The elements of $\widetilde{Y}'$ are derived from the application of KVL, KCL, and Ohm's law. From KCL at node i and the definitions of $\widetilde{V}_i'$ and $\widetilde{I}_i'$,

$$\widetilde{I}_{ik} = \frac{1}{aa^*}\widetilde{V}_i \left(\frac{\widetilde{y}_{ik}^{\mathrm{Sh}}}{2} + \widetilde{y}_{ik} \right) - \frac{1}{a^*}\widetilde{V}_k\widetilde{y}_{ik}. \tag{47}$$

Similarly, at bus k,

$$\widetilde{I}_{ki} = -\frac{1}{a}\widetilde{V}_i\widetilde{y}_{ik} + \widetilde{V}_k \left(\frac{\widetilde{y}_{ik}^{\mathrm{Sh}}}{2} + \widetilde{y}_{ik} \right). \tag{48}$$
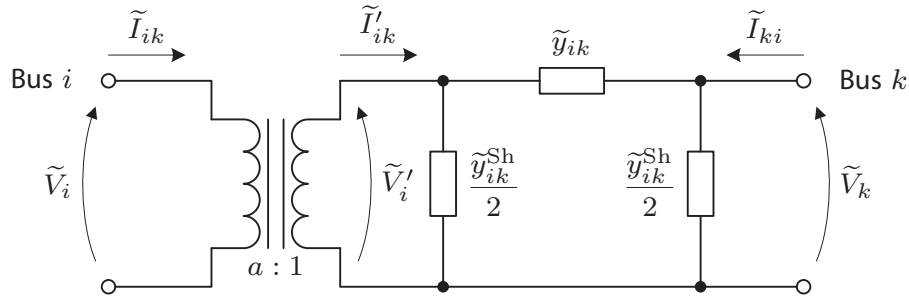
Figure 3. Generalized Π branch model, including off-nominal turns ratio.

Rearranging Equations (47) and (48) to form a matrix equation yields $\widetilde{Y}'$,

$$\begin{pmatrix} \widetilde{I}_{ik} \\ \widetilde{I}_{ki} \end{pmatrix} = \begin{pmatrix} \dfrac{1}{aa^*}\left(\dfrac{\widetilde{y}_{ik}^{\mathrm{Sh}}}{2} + \widetilde{y}_{ik}\right) & -\dfrac{1}{a^*}\widetilde{y}_{ik} \\ -\dfrac{1}{a}\widetilde{y}_{ik} & \dfrac{\widetilde{y}_{ik}^{\mathrm{Sh}}}{2} + \widetilde{y}_{ik} \end{pmatrix} \begin{pmatrix} \widetilde{V}_i \\ \widetilde{V}_k \end{pmatrix} = \widetilde{Y}'\begin{pmatrix} \widetilde{V}_i \\ \widetilde{V}_k \end{pmatrix}. \tag{49}$$

When constructing the full admittance matrix $\widetilde{Y}$, the corrected relationships of Equation (49) must be preserved. This is done via appropriate substitutions in Equation (45); Section 4.2 gives formulas for the resulting admittance matrix entries. A branch with off-nominal magnitude only (real valued a) leaves $\widetilde{Y}$ a symmetric matrix, but a phase-shifting transformer (complex a) does not.

4.1.1. Transmission lines and cables

The line characteristics for transmission lines and cables are most often specified as a series impedance $R_{ik} + jX_{ik}$ and a branch shunt admittance jb_{ik}^{Sh}, which is sometimes given as "line charging" reactive power. The Π branch series admittance $\widetilde{y}_{ik}$ for inclusion in $\widetilde{Y}$ is then

$$\widetilde{y}_{ik} = \frac{1}{R_{ik} + jX_{ik}} = \frac{R_{ik}}{R_{ik}^2 + X_{ik}^2} - j\frac{X_{ik}}{R_{ik}^2 + X_{ik}^2}. \tag{50}$$

As is typical for Π branch models, shunt susceptance b_{ik}^{Sh} is divided into two equal parts that are applied to the buses at each end of the branch. For short lines, branch shunt susceptance is negligible and therefore is usually omitted. Transmission lines and cables have nominal turns ratios: $T = 1.0$ and $\varphi = 0$.

4.1.2. Transformers

Like cables, power systems transformers have a series impedance $R_{ik} + jX_{ik}$ that models the electrical characteristics of the transformer windings. In PF analysis, however, the transformer series resistance is often neglected, yielding $\widetilde{y}_{ik} = -j/X_{ik}$. Although transformer models may also include a shunt admittance $\widetilde{y}_{ik}^{\mathrm{Sh}}$ that represents the losses and magnetizing characteristics of the transformer core, this shunt admittance is nearly always neglected as well.

Off-nominal transformers have either $T \neq 1$ and/or $\varphi \neq 0$. In OPF, both T and φ may be control variables: controllable T models an on-load tap changer, while controllable φ models a phase-shifting transformer.

4.2. Construction equations for admittance matrix

Any branch model may be distilled into a generic series admittance $\widetilde{y}_{ik}$, shunt admittance $\widetilde{y}_{ik}^{\mathrm{Sh}}$, and complex turns ratio (nominal or off-nominal) $a_{ik} = T_{ik}e^{j\varphi_{ik}}$. Using Equation (46) and incorporating the corrected off-nominal voltage–current relationships introduced in Section 4.1, the entries of $\widetilde{Y}$ become

$$\widetilde{Y}_{ii} = \widetilde{y}_i^{\mathrm{S}} + \sum_{k:(i,k)\in\mathbf{L}} \frac{1}{|a_{ik}|^2}\left(\widetilde{y}_{ik} + \frac{1}{2}\widetilde{y}_{ik}^{\mathrm{Sh}}\right) + \sum_{k:(k,i)\in\mathbf{L}}\left(\widetilde{y}_{ki} + \frac{1}{2}\widetilde{y}_{ki}^{\mathrm{Sh}}\right), \tag{51}$$

$$\widetilde{Y}_{ik} = -\sum_{k:(i,k)\in\mathbf{L}} \frac{1}{a_{ik}^*}\widetilde{y}_{ik} - \sum_{k:(k,i)\in\mathbf{L}} \frac{1}{a_{ik}}\widetilde{y}_{ki}, \quad i \neq k, \tag{52}$$

where $a_{ik} = 1$ for any branch with a nominal turns ratio. Equations (51) and (52) may be separated into real and imaginary parts using the definition $\widetilde{Y} = G + jB$ and the identity $a_{ik} = T_{ik}\left(\cos\varphi_{ik} + j\sin\varphi_{ik}\right)$,

$$G_{ii} = g_i^{\mathrm{S}} + \sum_{k:(i,k)\in\mathbf{L}} \frac{1}{T_{ik}^2}\left(g_{ik} + \frac{1}{2}g_{ik}^{\mathrm{Sh}}\right) + \sum_{k:(k,i)\in\mathbf{L}}\left(g_{ki} + \frac{1}{2}g_{ki}^{\mathrm{Sh}}\right), \tag{53}$$

$$G_{ik} = -\sum_{k:(i,k)\in\mathbf{L}} \frac{1}{T_{ik}}\left(g_{ik}\cos\varphi_{ik} - b_{ik}\sin\varphi_{ik}\right)$$
$$- \sum_{k:(k,i)\in\mathbf{L}} \frac{1}{T_{ki}}\left(g_{ki}\cos\varphi_{ki} + b_{ki}\sin\varphi_{ki}\right), \quad i \neq k \tag{54}$$

$$B_{ii} = b_i^{\mathrm{S}} + \sum_{k:(i,k)\in\mathbf{L}} \frac{1}{T_{ik}^2}\left(b_{ik} + \frac{1}{2}b_{ik}^{\mathrm{Sh}}\right) + \sum_{k:(k,i)\in\mathbf{L}}\left(b_{ki} + \frac{1}{2}b_{ki}^{\mathrm{Sh}}\right), \tag{55}$$

$$B_{ik} = -\sum_{k:(i,k)\in\mathbf{L}} \frac{1}{T_{ik}}\left(g_{ik}\sin\varphi_{ik} + b_{ik}\cos\varphi_{ik}\right)$$
$$- \sum_{k:(k,i)\in\mathbf{L}} \frac{1}{T_{ki}}\left(-g_{ki}\sin\varphi_{ki} + b_{ki}\cos\varphi_{ki}\right), \quad i \neq k. \tag{56}$$

Appendix D describes how to obtain the required parameters for constructing the admittance matrix from publicly available data sources.

5. The PF equations

The AC power flow equations transform the complex-domain matrix function (2) into a set of real-valued simultaneous equations suitable for inclusion in mathematical programming formulations. The most prevalent and compact form of the PF equations is the bus injection model. However, the less compact

branch flow model also describes Equation (2) and has several advantages with respect to convex relaxation of OPF problems.

5.1. Bus injection model

The bus injection model is usually synonymous with the term "AC power flow equations" and provides a compact representation of power system behavior in terms of the real and reactive power injection at each system bus. Use of the bus injection model is ubiquitous in conventional PF and in the early OPF literature.

For a given $\widetilde{Y}$, Equation (2) may be decomposed into a set of equations for the real and reactive power injections by evaluating the real and imaginary parts of S, respectively. The resulting pair of equations may be written in several equivalent forms depending on whether the voltages and admittance matrix elements are expressed in polar or rectangular coordinates. In the literature, the most common forms of the AC PF equations are, in order, as follows.

1. Selection of polar coordinates for voltage, $\widetilde{V}_i = V_i \angle \delta_i$, and rectangular coordinates for admittance, $\widetilde{Y}_{ik} = G_{ik} + jB_{ik}$:

$$P_i(V, \delta) = V_i \sum_{k=1}^{N} V_k \big(G_{ik} \cos(\delta_i - \delta_k) + B_{ik} \sin(\delta_i - \delta_k) \big) \quad \forall i \in \mathbf{N}, \quad (57)$$

$$Q_i(V, \delta) = V_i \sum_{k=1}^{N} V_k \big(G_{ik} \sin(\delta_i - \delta_k) - B_{ik} \cos(\delta_i - \delta_k) \big) \quad \forall i \in \mathbf{N}. \quad (58)$$

2. Selection of polar coordinates for voltage, $\widetilde{V}_i = V_i \angle \delta_i$, and polar coordinates for admittance, $\widetilde{Y}_{ik} = Y_{ik} \angle \theta_{ik}$:

$$P_i(V, \delta) = V_i \sum_{k=1}^{N} V_k Y_{ik} \cos(\delta_i - \delta_k - \theta_{ik}) \quad \forall i \in \mathbf{N}, \quad (59)$$

$$Q_i(V, \delta) = V_i \sum_{k=1}^{N} V_k Y_{ik} \sin(\delta_i - \delta_k - \theta_{ik}) \quad \forall i \in \mathbf{N}. \quad (60)$$

3. Selection of rectangular coordinates for voltage, $\widetilde{V}_i = E_i + jF_i$, and rectangular coordinates for admittance, $\widetilde{Y}_{ik} = G_{ik} + jB_{ik}$:

$$P_i(E, F) = \sum_{k=1}^{N} G_{ik}(E_i E_k + F_i F_k) + B_{ik}(F_i E_k - E_i F_k) \quad \forall i \in \mathbf{N}, \quad (61)$$

$$Q_i(E, F) = \sum_{k=1}^{N} G_{ik}(F_i E_k - E_i F_k) - B_{ik}(E_i E_k + F_i F_k) \quad \forall i \in \mathbf{N}. \quad (62)$$

Power systems texts (Wood and Wollenberg, 1996; Glover et al., 2008; Zhu, 2009) provide exact derivations of these three forms of the AC PF equations. (The fourth form—selection of rectangular coordinates for voltage and polar coordinates for admittance—is theoretically possible but has no advantages for practical use.) Each form of the equations involves real-valued quantities only. However, all forms are equivalent and give the exact solution to the PF under the analysis assumptions outlined in Appendix B.3.

The bus injection model of the AC PF equations yields exactly $2N$ simultaneous equations in $4N$ variables. Of these, only $N + M - 1$ equations in are needed for conventional PF. Despite the equations' nonlinearity and complexity, efficient solution methods exist for the conventional PF problem (see Section 6.1).

5.2. Branch flow model

The branch flow model is an alternative form of the PF equations that expresses the real and reactive PF in each system branch, as derived from Equation (44). Baran and Wu (1989a, 1989b) originated this model as part of an optimal capacitor placement problem in radial distribution systems, although earlier researchers had used similar, linear network flow models derived from DC PF (Section 5.3; Azevedo et al. (2010)). The branch flow model has received considerable recent interest because it offers advantages for convex relaxation of OPF problems (Farivar and Low, 2013a, 2013b).

Low (2013) summarizes the branch flow model using three sets of complex equations

$$\widetilde{V}_i - \widetilde{V}_k = \widetilde{Z}_{ik} \widetilde{I}_{ik} \quad \forall (i, k) \in \mathbf{L}, \quad (63)$$

$$S_{ik} = \widetilde{V}_i \widetilde{I}_{ik}^* \quad \forall (i, k) \in \mathbf{L}, \quad (64)$$

$$S_i = \sum_{k:(i,k)\in\mathbf{L}} S_{ik} - \sum_{k:(i,k)\in\mathbf{L}} \left(S_{ki} - \widetilde{Z}_{ki} |\widetilde{I}_{ki}|^2 \right) + (\widetilde{y}_i^S)^* |\widetilde{V}_i|^2 \quad \forall i \in \mathbf{N} \quad (65)$$

in which $\widetilde{Z}_{ik} = 1/\widetilde{y}_{ik}$ is the complex series impedance of each system branch. (Note that Equations (63) to (65) neglect branch shunt admittances and off-nominal turns ratios.) The system variables are $2L$ real-valued components of directed branch currents $i \to k$, $2L$ directed branch real and reactive power flows $i \to k$, N bus voltage magnitudes, N bus voltage angles, and $2N$ bus real and reactive power injections, for a total of $4N + 4L$ variables. Similarly, there are $2L$ directed branch current definitions $i \to k$, $2L$ directed branch real and reactive power definitions $i \to k$, and $2N$ bus power balance equations, for a total of $2N + 4L$ simultaneous equations. As with the bus injection model, the system is underdetermined by exactly $2N$ variables. However, the dimensionality of the system of equations is considerably larger.

Frank and Rebennack (2015) present an alternative form of the branch flow model that (i) uses rectangular coordinates for the bus voltages and (ii) substitutes the real and reactive PF at the receiving of each branch as variables in place of the branch currents. The branch power definitions follow directly from Equation (49) and the definition of complex power,

$$P_{ik} = \frac{1}{T_{ik}^2} \left(g_{ik} + \frac{g_{ik}^S}{2} \right) (E_i^2 + F_i^2) + \frac{1}{T_{ik}} \left(-g_{ik} \cos \varphi_{ik} + b_{ik} \sin \varphi_{ik} \right) (E_i E_k + F_i F_k)$$

$$+ \frac{1}{T_{ik}} \left(g_{ik} \sin \varphi_{ik} + b_{ik} \cos \varphi_{ik} \right) \left(E_i F_k - F_i E_k \right)$$

$$\forall \, (i, k) \in \mathbf{L}, \quad (66)$$

$$P_{ki} = \left(g_{ik} + \frac{g_{ik}^{\mathrm{S}}}{2} \right) \left(E_k^2 + F_k^2 \right)$$

$$+ \frac{1}{T_{ik}} \left(-g_{ik} \cos \varphi_{ik} - b_{ik} \sin \varphi_{ik} \right) \left(E_i E_k + F_i F_k \right)$$

$$+ \frac{1}{T_{ik}} \left(g_{ik} \sin \varphi_{ik} - b_{ik} \cos \varphi_{ik} \right) \left(E_i F_k - F_i E_k \right)$$

$$\forall \, (i, k) \in \mathbf{L}, \quad (67)$$

$$Q_{ik} = -\frac{1}{T_{ik}^2} \left(b_{ik} + \frac{b_{ik}^{\mathrm{S}}}{2} \right) \left(E_i^2 + F_i^2 \right)$$

$$+ \frac{1}{T_{ik}} \left(g_{ik} \sin \varphi_{ik} + b_{ik} \cos \varphi_{ik} \right) \left(E_i E_k + F_i F_k \right)$$

$$+ \frac{1}{T_{ik}} \left(g_{ik} \cos \varphi_{ik} - b_{ik} \sin \varphi_{ik} \right) \left(E_i F_k - F_i E_k \right)$$

$$\forall \, (i, k) \in \mathbf{L}, \quad (68)$$

$$Q_{ki} = -\left(b_{ik} + \frac{b_{ik}^{\mathrm{S}}}{2} \right) \left(E_k^2 + F_k^2 \right)$$

$$+ \frac{1}{T_{ik}} \left(-g_{ik} \sin \varphi_{ik} + b_{ik} \cos \varphi_{ik} \right) \left(E_i E_k + F_i F_k \right)$$

$$+ \frac{1}{T_{ik}} \left(-g_{ik} \cos \varphi_{ik} - b_{ik} \sin \varphi_{ik} \right) \left(E_i F_k - F_i E_k \right)$$

$$\forall \, (i, k) \in \mathbf{L}. \quad (69)$$

Bus power balance equations (65) are still required but instead take the form

$$P_i = \sum_{k:(i,k)\in\mathbf{L}} P_{ik} + \sum_{k:(i,k)\in\mathbf{L}} P_{ik} \forall \, i \in \mathbf{N}, \quad (70)$$

$$Q_i = \sum_{k:(i,k)\in\mathbf{L}} Q_{ik} + \sum_{k:(i,k)\in\mathbf{L}} Q_{ik} \forall \, i \in \mathbf{N}. \quad (71)$$

Unlike Equations (63) to (65), Equations (66) to (71) do include the effects of branch shunt admittances and off-nominal turns ratios. The system of equations still contains $4N + 4L$ variables ($2N$ bus voltage components, $2N$ bus real and reactive power injections, and $4L$ directed branch real and reactive power flows) and $2N + 4L$ simultaneous equations.

5.3. DC PF

The AC PF equations are nonlinear. For conventional PF, this nonlinearity requires the use of an iterative numerical method; for OPF it implies both a nonlinear formulation and non-convexity in the feasible region. In order to simplify the system representation, power systems engineers have developed a linear approximation to the PF equations. This approximation is called

DC PF—so named because the equations resemble the PF in a direct current (DC) network. However, the DC PF equations still model an AC power system.

The conventional development of the DC PF equations requires several assumptions regarding the power system (Rau, 2003b; Zhu, 2009):

1. All system branch resistances are approximately zero; that is, the transmission system is assumed to be lossless. As a result, all $\theta_{ik} = \pm 90°$ and all $G_{ik} = 0$.
2. The differences between adjacent bus voltage angles are small, such that $\sin(\delta_i - \delta_k) \approx \delta_i - \delta_k$ and $\cos(\delta_i - \delta_k) \approx 1$.
3. The system bus voltages are approximately equal to 1.0. This assumption requires that there is sufficient reactive power generation in the system to maintain a level voltage profile.
4. Reactive PF is neglected.

Applying these assumptions to Equation (57) produces the DC power flow equation

$$P_i(\delta) \approx \sum_{k=1}^{N} B_{ik} (\delta_i - \delta_k). \quad (72)$$

Under normal operating conditions, DC PF models real power transfer quite accurately. It has been successfully used in many OPF applications that require rapid and robust solutions, including in commercial software. However, the assumptions required for DC PF can lead to significant errors for stressed systems.

Neglecting off-nominal turns ratios, the exact equation for branch power transfer is

$$P_{ik} = g_{ik} V_i^2 - g_{ik} V_i V_k \cos (\delta_i - \delta_k) - b_{ik} V_i V_k \sin (\delta_i - \delta_k), \quad (73)$$

cf. Equation (57), and the DC PF approximation is

$$P_{ik} \approx -b_{ik} (\delta_i - \delta_k). \quad (74)$$

The b_{ik} term dominates the exact expression because $V_i^2 \approx V_i V_k \cos (\delta_i - \delta_k)$ and therefore the first two terms in Equation (73) largely cancel. We observe that Equation (74) overestimates the magnitude of the branch power transfer (73) if

(i) The bus voltages at either end of the branch are depressed relative to the assumed value of 1.0 p.u.; or
(ii) The angle difference between the buses is too large.

Observation (ii) follows from the relationship $|\sin (\delta_i - \delta_k)| \leq |\delta_i - \delta_k|$. Depressed voltages and larger than normal angle differences are common in stressed power systems. In particular, large differences in voltage in different areas of the system can lead to significant error (Stott et al., 2009). Therefore, the DC PF equations should not be used for OPF under stressed system conditions unless they have been carefully evaluated for accuracy in the system under test.

As an example, consider an arbitrary transmission line from bus i to bus k with series admittance $0.05 - j2.0$. Let $\widetilde{V}_i = 0.95\angle 0°$ and $\widetilde{V}_k = 0.90\angle -20°$. (Although these numbers do not represent normal operation, they are plausible for a stressed power system. Operating voltages as low as 0.9 p.u. are allowable in emergency conditions, and angle differences of up to $\pm 30°$ can occur on long, heavily loaded transmission lines.) The exact

power transfer for this line is

$$P_{ik} = 0.05 \times 0.95^2 - 0.05 \times 0.95 \times 0.90 \cos{(0° + 20°)}$$
$$-2.0 \times 0.95 \times 0.90 \sin{(0° + 20°)} = 0.590 \text{ p.u.}$$

The DC approximate power transfer is

$$P_{ik} \approx -2.0 \sin{(0° + 20°)} \approx 0.684 \text{ p.u.}$$

The error in the approximate power transfer is 16%; most of this error is attributable to the voltage difference. In systems with severely depressed voltages, large absolute errors in line power are typical, although the relative error in the proportion of total power flowing in each line may be much smaller (Stott *et al.*, 2009).

Even under normal operation, the approximation of a lossless transmission network can also lead to significant errors in generator scheduling, branch PF estimates, and marginal fuel cost estimates. Power transfer errors for certain critically loaded branches can be much higher than the average branch error. Therefore, in practical DC PF models an estimate of the losses must be reintroduced using approximate methods, especially if the network is large (Stott *et al.*, 2009). For further discussion regarding the advantages and disadvantages of DC PF, including loss approximation methods, we refer the interested reader to Rau (2003a) and Stott *et al.* (2009). Throughout the rest of this article, we use the AC PF equations.

5.4. The PF equations as constraints

In OPF, the PF equations form the core of the set of equality constraints. A large majority of OPF formulations use the bus injection model because (i) it is more compact and (ii) it more closely resembles conventional PF, which facilitates the development of tailored algorithms. The advantages of the branch flow model are the explicit modeling of branch power flows, which facilitates inclusion of transmission capacity constraints, and that the form of the equations enables certain convex relaxations.

Traditionally, the branch impedances and elements of $\widetilde{Y}$ are considered constant: most algorithmic development and analysis in the engineering literature assumes constant $\widetilde{Y}$. In newer OPF formulations $\widetilde{Y}$ may also contain control (decision) variables due to phase-shifting or tap-changing transformers, which significantly complicates the problem by introducing bilinear, trilinear, or other nonlinear terms.

5.4.1. Considerations for the bus injection model

The key consideration when using the bus injection model is the choice of polar or rectangular coordinates for voltage. The advantage of voltage polar coordinates is that constraints on the voltage magnitude can be enforced directly,

$$V_i \geq V_i^{\min},$$
$$V_i \leq V_i^{\max}.$$

In voltage rectangular coordinates, on the other hand, voltage magnitude limits require the functional inequality constraints

$$\sqrt{E_i^2 + F_i^2} \geq V_i^{\min},$$
$$\sqrt{E_i^2 + F_i^2} \leq V_i^{\max}.$$

Similarly, if the voltage magnitude is fixed (for instance at a PV bus; see Section 2.3), then in polar coordinates V_i can be replaced with a constant value. In rectangular coordinates, however, a fixed voltage magnitude requires the equality constraint

$$\sqrt{E_i^2 + F_i^2} = V_i.$$

Thus, for a fixed voltage magnitude, use of voltage polar coordinates leads to a reduction of variables whereas the use of voltage rectangular coordinates leads to an increase in (nonlinear, non-convex) equality constraints. For this reason, polar coordinates are preferred both for conventional PF and most OPF formulations.

There is, however, one compelling reason to use voltage rectangular coordinates: expressing voltage in rectangular coordinates eliminates trigonometric functions from the PF equations. The resulting PF Equations (61) and (62) are quadratic, which presents several advantages (Torres and Quintana, 1998):

1. The elimination of trigonometric functions speeds evaluation of the equations.
2. The second order Taylor series expansion of a quadratic function is exact; this yields an efficiency advantage in higher-order interior-point algorithms for OPF.
3. The Hessian matrix for a quadratic function is constant and must be evaluated only once. This simplifies the application of Newton's method to the Karush–Kuhn–Tucker (KKT) conditions of the OPF formulation.
4. If the side constraints are also quadratic, then the entire OPF problem becomes a Quadratically Constrained Program, although it remains non-convex. This enables the use of specialized solution algorithms.

In some cases, these computational advantages outweigh the disadvantages associated with increased dimensionality and enforcing voltage magnitude constraints. Table 2 summarizes the differences between the two voltage coordinate choices.

For the admittance matrix elements, rectangular coordinates (56) and (57) are typically favored because they facilitate the use of certain approximations in fast-decoupled solution methods for conventional PF (Zhu, 2009). These approximations are also useful in the development of the DC PF equations (Section 5.3). Finally, rectangular coordinates facilitate the inclusion of transformer voltage ratios and phase angles as decision variables. However, none of these advantages strongly affects the AC PF equations as implemented in many OPF formulations, and some models use the polar form of the Equations (59) and (60).

Table 2. Comparison of the selection of voltage polar coordinates versus voltage rectangular coordinates for the power flow equations. Bold entries indicate the more favorable characteristic.

	Polar coords.	Rectangular coords.
Number of variables in conventional PF	$N + M - 1$	$2N - 2$
Voltage magnitude limits	**Simple bounds**	Nonlinear functional inequality constraint
Fixed voltage magnitude	**Variable elimination by substitution**	Nonlinear functional equality constraint
Nature of PF equations	Trigonometric	**Quadratic**
First derivative of PF equations	Trigonometric	**Linear**
Second derivative of PF equations	Trigonometric	**Constant**

5.4.2. Considerations for the branch flow model

As solving OPF problems is NP-hard, convex relaxations are of particular interest, especially when conditions are known that cause these relaxations to be exact. There are several different approaches to convexify the OPF problem, dependent on the formulation used (Low, 2013). Examples of such relaxations include semidefinite programming, second-order cone programming, and convex Lagrangian dual. Quite surprisingly, the exactness of some of these relaxations has been proven for radial networks (under mild conditions). However, for mesh networks under the classic bus injection model, examples with large duality gap have been published and, as a consequence, the relaxations are no longer exact.

In contrast, the branch flow model allows for exact relaxations and convexifications for both radial and mesh networks (under mild conditions, for instance, no upper bounds on loads; Farivar and Low (2013a, 2013b)). Moreover, the interpretation of the decision variables in a branch flow model (for instance, branch power and current flows) is more intuitive compared with the semidefinite matrix and second-order cone programming relaxations and tend to be numerically more stable compared with second-order cone programming relaxations for the bus injection models (Low, 2014).

If the rectangular coordinate branch flow model (66)–(69) is used, then a linear relaxation may be obtained by introducing auxiliary variables for the quadratic terms and subsequently applying the McCormick inequalities (Frank and Rebennack, 2015). Although the relaxation is not exact, in practice it can be made relatively tight by introducing tailored cuts that constrain the branch power flows. The linear relaxation allows rapid generation of lower bounds on the objective function value and facilitates mixed integer-linear relaxations for more complex OPF variants.

5.5. Side constraints

In addition to the PF equations, a typical OPF problem includes a number of side constraints. The simplest of these are box constraints (8) to (11) that define the upper and lower limits for the controllable generation, the bus voltage magnitudes, and the bus voltage angles.

If the system contains controllable phase-shifting or tap-changing transformers, then the corresponding phase angles φ and tap ratios T are introduced into the set of control variables. The control variable vector u becomes

$$u = \left(P^{\mathrm{G}}_{i:i\in\mathbf{G}}, Q^{\mathrm{G}}_{i:i\in\mathbf{G}}, \varphi_{ik:ik\in\mathbf{H}}, T_{ik:ik\in\mathbf{K}} \right),$$

where $\mathbf{H}$ and $\mathbf{K}$ are the sets of branches with controllable-phase shifting transformers and tap-changing transformers, respectively. Since φ and T alter the elements of admittance matrix $\widetilde{Y}$, the left-hand sides of Equations (6) and (7) become functions of φ and T: $P_i(V, \delta, \varphi, T)$ and $Q_i(V, \delta, \varphi, T)$, respectively. The formulation is also augmented with bound constraints on the phase angles

$$\varphi^{\min}_{ik} \leq \varphi_{ik} \leq \varphi^{\max}_{ik} \qquad \forall\, ik \in \mathbf{H} \tag{75}$$

and the tap ratios

$$T^{\min}_{ik} \leq T_{ik} \leq T^{\max}_{ik} \qquad \forall\, ik \in \mathbf{K}. \tag{76}$$

Adding controllable phase-shifting or tap-changing transformers significantly complicates the OPF problem, rendering many common approximations and relaxations invalid. Some OPF research has therefore explored alternative models for controllable transformers and other advanced PF control devices, such as the inclusion of auxiliary buses or idealization of such transformers as controlled power injections (Acha *et al.*, 2000; Lehmköster, 2002; Xiao *et al.*, 2002).

Many recent OPF formulations also include line limits; that is, upper bounds on the branch current magnitudes. Since line current is voltage dependent, an exact bound requires a function inequality constraint. By Ohm's law, the current magnitude in branch ik is

$$I_{ik} = \left| \widetilde{V}_i - \widetilde{V}_k \right| y_{ik},$$

in which y_{ik} is the magnitude of the branch admittance. Thus, one version of the exact bound is

$$\left| \widetilde{V}_i - \widetilde{V}_k \right| y_{ik} \leq I^{\max}_{ik},$$

$$\Leftrightarrow \quad \sqrt{(V_i \cos \delta_i - V_k \cos \delta_k)^2 + (V_i \sin \delta_i - V_k \sin \delta_k)^2} \leq \frac{I^{\max}_{ik}}{y_{ik}},$$

$$\Leftrightarrow \quad (V_i \cos \delta_i - V_k \cos \delta_k)^2$$
$$+ (V_i \sin \delta_i - V_k \sin \delta_k)^2 \leq \frac{\left(I^{\max}_{ik}\right)^2}{y^2_{ik}} \quad \forall\, ik \in \mathbf{L}. \tag{77}$$

(For branches with off-nominal turns ratios, the tap bus voltage V_i and angle δ_i in Equation (77) must be corrected for the off-nominal turns ratio. In this case, V_i is replaced by $V'_i = V_i / T_{ik}$ and δ_i is replaced by $\delta'_i = \delta_i - \varphi_{ik}$.)

Rather than bounding the square of the current as is given in Equation (77), most formulations instead bound the real and reactive PF in the line

$$P^2_{ik} + Q^2_{ik} \leq \left(S^{\max}_{ik} \right)^2.$$

In almost all cases, this simplification is sufficiently accurate.

6. Solution methods

In this section, we provide a concise discussion of OPF solution methods and their relationship to conventional PF. As many OPF algorithms rely on or incorporate aspects of conventional PF algorithms, we summarize conventional PF solution methods first.

6.1. Solution methods for conventional PF

Recall from Section 2.3 that conventional PF seeks a numerical solution to the exactly determined system of complex nonlinear equations

$$S = \widetilde{V} \circ \left(\widetilde{Y} \widetilde{V} \right)^*.$$

Newton's method is typically used to solve this system and is fully described in power systems texts (Wood and Wollenberg, 1996; Glover *et al.*, 2008; Zhu, 2009). Here, we summarize the solution of the AC PF equations with voltage polar coordinates. The solution method for voltage rectangular coordinates is similar; Zhu (2009) provides a good summary.

The first-order Taylor series approximation of Equations (57) and (58) about the current estimate of V and δ yields

$$\begin{pmatrix} \Delta P \\ \Delta Q \end{pmatrix} \approx \begin{pmatrix} \dfrac{\partial P}{\partial \delta} & \dfrac{\partial P}{\partial V} \\ \dfrac{\partial Q}{\partial \delta} & \dfrac{\partial Q}{\partial V} \end{pmatrix} \begin{pmatrix} \Delta \delta \\ \Delta V \end{pmatrix},$$

$$\approx J \begin{pmatrix} \Delta \delta \\ \Delta V \end{pmatrix}, \tag{78}$$

in which J is the Jacobian matrix of system (57)–(58). At each iteration, the mismatches in the PF equations are

$$\Delta P_i = \left(P_i^{\mathrm{G}} - P_i^{\mathrm{L}} \right) - P_i \left(V, \delta \right), \tag{79}$$

$$\Delta Q_i = \left(Q_i^{\mathrm{G}} - Q_i^{\mathrm{L}} \right) - Q_i \left(V, \delta \right). \tag{80}$$

Newton's method consists of iteratively solving Equation (78) for the $\Delta \delta$ and ΔV required to correct the mismatch in the PF equations computed from Equations (79) and (80). Newton's method is locally quadratically convergent. Therefore, given a sufficiently good starting point, the method reliably finds the correct solution to the PF equations. However, convergence is not guaranteed: the method can fail to converge if the starting voltage estimate is poor, as can occur in a stressed power system (Bienstock, 2013). To address the convergence issue, a few researchers have applied globally convergent solution methods (Han, 1977) to conventional PF and OPF, including the application of homotopy (Cvijić et al., 2012), a backtracking line search method (Pajic and Clements, 2005), and trust region methods (Pajic and Clements, 2005; Sousa et al., 2011). Such methods are generally robust with respect to poor quality starting points but incur a significant computational penalty.

6.1.1. Decoupled PF algorithms

In practical power systems, real power injections are strongly coupled to voltage angles and reactive power injections are strongly coupled to voltage magnitudes. Conversely, real power injections are weakly coupled to voltage magnitudes and reactive power injections are weakly coupled to voltage angles. This feature has led to the development of decoupled solution methods for the PF equations (Glover et al., 2008; Zhu, 2009). The most basic decoupling method is to use a set of approximate Taylor series expansions of the form

$$\Delta P \approx \frac{\partial P}{\partial \delta} \Delta \delta,$$

$$\Delta Q \approx \frac{\partial Q}{\partial V} \Delta V.$$

This allows the use of separate Newton updates for δ and V with correspondingly smaller matrices—a significant computational advantage.

Although decoupled PF uses an approximate update method, it still computes exact real and reactive power mismatches ΔP and ΔQ from Equations (79) and (80) and updates both V and δ at each iteration. Decoupled PF therefore is locally convergent to the exact solution to the PF. However, due to the approximated Jacobian matrix, more iterations are required for convergence (Glover et al., 2008). Zhu (2009) discusses several decoupled PF variants in detail.

6.1.2. DC PF algorithms

In DC PF, there is no distinction between PV and PQ buses because all voltage magnitudes are considered to be 1.0 and reactive power is neglected. As with the AC PF, the slack bus angle is fixed. As the DC PF equations are linear, they may be solved directly for the voltage angles using

$$\delta = B^{-1} P.$$

(This is simply a solved matrix representation of Equation (72).)

6.2. Solution methods for OPF

The existing OPF literature describes an immense variety of approaches and solution methods. As mentioned in the Introduction, our intent in this article is to provide an operations researcher with sufficient information to formulate OPF problems, understand the challenges and open problems in the field, and comprehend the electrical engineering-dominated literature on OPF solution methods. Therefore, we refrain from summarizing the vast literature on tailored OPF solution methods and instead refer the reader to the two surveys (Frank et al., 2012a, 2012b). We do, however, highlight several popular methods and their relationship to conventional PF.

Many classic nonlinear optimization techniques have been applied to the OPF problem, including gradient descent methods, Newton's method, Sequential Linear Programming (SLP), and Sequential Quadratic Programming (SQP). Recall from Section 2.4 that many OPF algorithms partition the decision variables into a set of control variables u and a set of state variables x. At each search step, the algorithm fixes u and derives x by solving a conventional PF. When this approach is used, the Jacobian matrix J from conventional PF plays several important roles.

1. It provides the linearization of the PF equations required for SLP and SQP iterations.
2. It provides sensitivities in the PF injections with respect to the state variables.
3. It provides a direct calculation of portions of the Hessian matrix of the Lagrangian function for OPF algorithms based on Newton's method (see Sun et al. (1984)).
4. It is therefore often used to improve computational efficiency in computing the KKT conditions for the Lagrangian function.

More recently, nonlinear Interior-Point Methods (IPMs) and various convex relaxation approaches such as semidefinite programming have become popular for OPF (Frank et al., 2012a). Many such methods rely heavily on specific characteristics of the PF equations in order to establish convergence properties or evaluate the tightness of the relaxation. Many meta-heuristic methods and hybrid methods combining meta-heuristics with deterministic approaches have also been applied to OPF (Frank et al., 2012b). In the case of meta-heuristics, the typical approach is again to select a trial vector for u and compute the corresponding state vector x and objective function value using conventional PF.

6.3. Practical considerations

In our experience, there are several practical and computational aspects of OPF stemming from the power flow equations that can cause confusion or lead to solution errors. Two of these are the use of the per unit system and formats for the exchange of OPF data, discussed in Appendices C and D, respectively. We note several others here.

6.3.1. Decoupled solution methods for OPF

Like decoupled PF, decoupled OPF algorithms take advantage of the strong P–δ and Q–V relationships in the PF equations by formulating separate real and reactive OPF subproblems. These subproblems and their optima are assumed to be independent. Unlike decoupled PF, however, decoupled OPF solves the subproblems sequentially rather than simultaneously: the real subproblem solves for the optimal values of P and δ while holding Q and V constant, and the reactive subproblem solves for the optimal values of Q and V while holding P and δ constant (Sun et al., 1984; Contaxis et al., 1986). To enable this decomposition, decoupled OPF neglects the weak P–V and Q–δ relationships in the constraints, introducing slight errors in the computed power flows. Decoupled OPF is therefore distinctly different from decoupled PF in that the decoupled OPF solution is inexact.

The error in the decoupled OPF solution with respect to the true optimum is a function of the accuracy of the decoupling assumptions and can be significant if the system includes advanced control devices (Zhang, 2010). These assumptions should therefore be evaluated for accuracy if a decoupled OPF approach is considered. In the OPF literature, it is not always immediately apparent whether decoupled OPF is in use or whether a decoupled PF procedure is used within the solution algorithm for a coupled OPF. Due to the implications for the OPF solution quality, the careful reader should try to discern which is the case.

6.3.2. Degrees versus radians

Power systems engineers usually report angles in degrees, including in data files for OPF (see Appendix D). For computation, these angles must be converted to radians, for two reasons:

1. Nearly all optimization software and algebraic modeling languages—including AMPL and GAMS—implement trigonometric functions in radians, not degrees.
2. Even when using the DC PF equations (which require no trigonometric function evaluations), radians must be used due to the derivation of the equations. If degrees are used, the powers computed from DC PF will have a scaling error of $180/\pi$.

PF software typically handles these conversions transparently, accepting input and giving output in degrees. Thus, it can be difficult to remember that general-purpose optimization software requires an explicit conversion.

6.3.3. System initialization

In both conventional PF and OPF, the convergence of the PF equations depends strongly on the selection of a starting point.
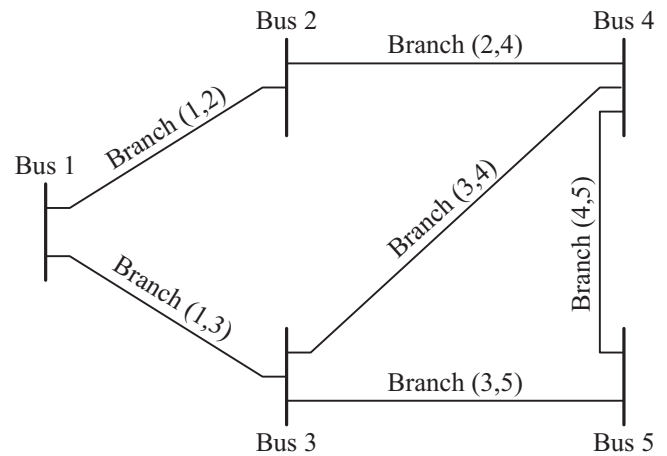

Figure 4. Bus and branch indices in an example five-bus electrical network.

Given a starting point far from the correct solution, the PF equations may converge to a meaningless solution or may not converge at all. In the absence of a starting point, standard practice is to initialize all voltage magnitudes to 1.0 p.u. and all voltage angles to zero; this is called a "cold start" or a "flat start." The alternative is a "warm start," in which the voltages and angles are initialized to the solution of a pre-solved power flow. Warm starts are often used in online OPF to minimize computation time and ensure that the search begins from the current system operating condition. Warm starts also aid the algorithm in converging to the nearest local minimum, which is often desirable during real-time operation of power systems.

If a good starting point is unavailable or the OPF algorithm encounters convergence problems, it is also possible to switch to a more robust solution method. Trust region methods and their variants coupled with IPMs are a popular and effective approach (Pajic and Clements, 2005; Wang et al., 2007; Sousa et al., 2011). The primary disadvantage of such methods is a significant computational penalty compared with their less-robust counterparts.

7. Numerical example

We now present a small numerical example to illustrate some key elements of a typical OPF formulation. The network of Fig. 4 provides the basis for the example OPF problem. It has $N = 5$ buses and $L = 6$ branches, with corresponding sets

$$\mathbf{N} = \{1, 2, 3, 4, 5\}$$

and

$$\mathbf{L} = \{(1, 2), (1, 3), (2, 4), (3, 4), (3, 5), (4, 5)\}.$$

Using this network, we derive the admittance matrix (Section 7.1), define the PF equations (Section 7.2), and develop the classic OPF problem and its optimal solution (Section 7.3).

7.1. Admittance matrix

Table 3 provides a set of branch data for the example system. Note that branch $(3, 4)$ is a phase-shifting transformer and branch $(4, 5)$ has an off-nominal voltage ratio. In addition to the

Table 3. Branch impedance data for the network of Fig. 4. All quantities except phase angles are given in per unit. Dots indicate nominal voltage ratios and phase angles.

From bus i	To bus k	Series resistance R_{ik}	Series reactance X_{ik}	Shunt susceptance b_{ik}^{Sh}	Voltage ratio T_{ik}	Phase angle φ_{ik}
1	2	0.000	0.300	0.000	.	.
1	3	0.023	0.145	0.040	.	.
2	4	0.006	0.032	0.010	.	.
3	4	0.020	0.260	0.000	.	$-3.0°$
3	5	0.000	0.320	0.000	0.98	.
4	5	0.000	0.500	0.000	.	.

branch data, bus 2 has a shunt susceptance of $j0.30$ pu and bus 3 has a shunt conductance of 0.05 pu.

To compute the admittance matrix for this system, we first compute the series admittance $\widetilde{y}_{ik}$ of each branch using Equation (50). For example, the series admittance of branch $(1, 3)$ is

$$\widetilde{y}_{13} = \frac{0.023}{0.023^2 + 0.145^2} - j\frac{0.145}{0.023^2 + 0.145^2} \approx 1.067 - j6.727.$$

The remaining branches have series admittances

$$\widetilde{y}_{12} \approx 0.000 - j3.333,$$
$$\widetilde{y}_{24} \approx 5.660 - j30.189,$$
$$\widetilde{y}_{34} \approx 0.294 - j3.824,$$
$$\widetilde{y}_{35} \approx 0.000 - j3.125,$$

and

$$\widetilde{y}_{45} \approx 0.000 - j2.000.$$

Next, we construct $\widetilde{Y}$ using Equations (51) and (52). For example, diagonal element $\widetilde{Y}_{33}$ consists of summing the admittances of branches $(1, 3)$, $(3, 4)$, and $(3, 5)$, plus the contributions of the shunt conductance at bus 3 and the shunt susceptance of branch $(1, 3)$. Branch admittances $\widetilde{y}_{34}$ and $\widetilde{y}_{35}$ have off-nominal turns ratios

$$a_{34} = 1.0e^{-j3.0°} \approx 0.999 - j0.052$$

and

$$a_{35} = 0.98e^{-j0.0°} = 0.980,$$

respectively. (Note that $a_{34}a_{34}^* = 1.0$ if rounding errors are neglected.) Therefore, matrix element $\widetilde{Y}_{33}$ is

$$\widetilde{Y}_{33} \approx (1.067 - j6.727) + j\frac{0.04}{2}$$
$$+ \frac{0.294 - j3.824}{(0.999 - j0.052)(0.999 + j0.052)} - \frac{j3.125}{0.980^2}$$
$$+ 0.05 \approx 1.41 - j13.78.$$

An example off-diagonal element is $\widetilde{Y}_{34}$, which from Equation (52) is

$$\widetilde{Y}_{34} \approx -\frac{0.294 - j3.824}{(0.999 + j0.052)} \approx -0.09 + j3.83.$$

The full admittance matrix is

$$\widetilde{Y} \approx \begin{pmatrix} 1.07 - j10.04 & 0.00 + j3.33 & -1.07 + j6.73 & 0 & 0 \\ 0.00 + j3.33 & 5.66 - j33.22 & 0 & -5.66 + j30.19 & 0 \\ -1.07 + j6.73 & 0 & 1.41 - j13.78 & -0.09 + j3.83 & 0.00 + j3.19 \\ 0 & -5.66 + j30.19 & -0.49 + j3.80 & 5.95 - j36.01 & 0.00 + j2.00 \\ 0 & 0 & 0.00 + j3.19 & 0.00 + j2.00 & 0.00 - j5.13 \end{pmatrix}.$$

7.2. PF equations

Using the previously developed admittance matrix, we can write the real and reactive PF equations for any bus in the five-bus example system. For example, from Equation (57), the real power injection at bus 1 is

$$P_1(V, \delta) = V_1 \sum_{k=1}^{5} V_k \big(G_{1k} \cos(\delta_1 - \delta_k) + B_{1k} \sin(\delta_1 - \delta_k) \big),$$
$$\approx 1.07V_1^2 \cos(\delta_1 - \delta_1) - 1.07V_1V_3 \cos(\delta_1 - \delta_3)$$
$$- 10.04V_1^2 \sin(\delta_1 - \delta_1)$$
$$+ 3.33V_1V_2 \sin(\delta_1 - \delta_2) + 6.73V_1V_3 \sin(\delta_1 - \delta_3),$$
$$\approx 1.07V_1^2 - 1.07V_1V_3 \cos(\delta_1 - \delta_3)$$
$$+ 3.33V_1V_2 \sin(\delta_1 - \delta_2) + 6.73V_1V_3 \sin(\delta_1 - \delta_3).$$

Similarly, from Equation (58), the reactive power injection at bus 1 is

$$Q_1(V, \delta) = V_1 \sum_{k=1}^{5} V_k \big(G_{1k} \sin(\delta_1 - \delta_k) - B_{1k} \cos(\delta_1 - \delta_k) \big),$$
$$\approx 1.07V_1^2 \sin(\delta_1 - \delta_1) - 1.07V_1V_3 \sin(\delta_1 - \delta_3)$$
$$+ 10.04V_1^2 \cos(\delta_1 - \delta_1)$$
$$- 3.33V_1V_2 \cos(\delta_1 - \delta_2) - 6.73V_1V_3 \cos(\delta_1 - \delta_3),$$
$$\approx -1.07V_1V_3 \sin(\delta_1 - \delta_3) + 10.04V_1^2$$
$$- 3.33V_1V_2 \cos(\delta_1 - \delta_2) - 6.73V_1V_3 \cos(\delta_1 - \delta_3).$$

7.3. OPF formulation and solution

We now develop the classic OPF formulation for the five-bus example system presented in Fig. 4, with the addition of two advanced control elements. The branch impedance data are as given in Table 3, except that we assign φ_{34} and T_{35} to be decision variables representing a phase-shifting transformer and an on-load tap changer, respectively. φ_{34} and T_{35} have limits

$$-30.0° \leq \varphi_{34} \leq 30.0°$$

and

$$0.95 \leq T_{35} \leq 1.05.$$

Tables 4 and 5 give the bus data (voltage limits, load, and generation). The system power base is 100 MW.

Table 4. Bus data for the network of Fig. 4. All quantities are given in per unit. Dots indicate zero values.

Bus i	Load real power P_i^L	Load reactive power Q_i^L	Min. bus voltage V_i^{min}	Max. bus voltage V_i^{max}
1	·	·	1.00	1.00
2	·	·	0.95	1.05
3	·	·	0.95	1.05
4	0.900	0.400	0.95	1.05
5	0.239	0.129	0.95	1.05

Table 5. Generator data for the network of Fig. 4. All quantities are given in per unit.

Bus i	Min. generator real power $P_i^{G,min}$	Max. generator real power $P_i^{G,max}$	Min. generator reactive power $Q_i^{G,min}$	Max. generator reactive power $Q_i^{G,max}$
1	$-\infty$	∞	$-\infty$	∞
3	0.10	0.40	−0.20	0.30
4	0.05	0.40	−0.20	0.20

Given this data, the sets defining the formulation are

$$\mathbf{N} = \{1, 2, 3, 4, 5\},$$
$$\mathbf{G} = \{1, 3, 4\},$$
$$\mathbf{L} = \{(1, 2), (1, 3), (2, 4), (3, 4), (3, 5), (4, 5)\},$$
$$\mathbf{H} = \{(3, 4)\},$$

and

$$\mathbf{K} = \{(3, 5)\}.$$

Let the three generator cost functions, in thousands of dollars, be

$$C_1\left(P_1^G\right) = 0.35 P_1^G,$$
$$C_3\left(P_3^G\right) = 0.20 P_3^G + 0.40\left(P_3^G\right)^2,$$
$$C_4\left(P_4^G\right) = 0.30 P_4^G + 0.50\left(P_4^G\right)^2,$$

in which the P_i^G are expressed in per-unit.

To develop the full formulation, it is first necessary to re-write $\widetilde{Y}$ as derived in Section 7.1 to explicitly include φ_{34} and T_{35}. Let

$$a_{34} = \cos\varphi_{34} + j\sin\varphi_{34}$$

and

$$a_{35} = T_{35}.$$

(Note that $a_{34}a_{34}^* = 1.0$, $1/a_{34} = \cos\varphi_{34} - j\sin\varphi_{34} = a_{34}^*$, and $1/a_{34}^* = \cos\varphi_{34} + j\sin\varphi_{34} = a_{34}$.) Then, using Equations (51) and (52) and simplifying,

$$\widetilde{Y}_{33} = 1.41 - j10.53 - j\frac{1}{T_{35}^2} \times 3.13,$$

$$\widetilde{Y}_{34} = -0.29\cos\varphi_{34} - 3.82\sin\varphi_{34}$$
$$+ j\left(3.82\cos\varphi_{34} - 0.29\sin\varphi_{34}\right),$$

$$\widetilde{Y}_{43} = -0.29\cos\varphi_{34} + 3.82\sin\varphi_{34}$$
$$+ j\left(3.82\cos\varphi_{34} + 0.29\sin\varphi_{34}\right),$$

$$\widetilde{Y}_{35} = j\frac{1}{T_{35}} \times 3.13,$$

and

$$\widetilde{Y}_{53} = j\frac{1}{T_{35}} \times 3.13.$$

$\widetilde{Y}_{44}$, $\widetilde{Y}_{55}$, and the other remaining matrix elements are unchanged.

Bus 1 is the system slack bus and therefore $\widetilde{V}_1$ is fixed to $1.0\angle 0.0°$. To construct the formulation, we round all numerical values to two decimal places. (This rounding does not affect model feasibility because sufficient degrees of freedom exist in the state variables.) Following Equations (5) to (11), (75), and (76), the full formulation is

$$\min \quad 0.35 P_1^G + 0.20 P_3^G + 0.40\left(P_3^G\right)^2 + 0.30 P_4^G + 0.50\left(P_4^G\right)^2,$$

s.t.
$$P_1^G = 1.07 - 1.07 V_3\cos\left(-\delta_3\right) + 3.33 V_2\sin\left(-\delta_2\right)$$
$$+ 6.73 V_3\sin\left(-\delta_3\right),$$

$$0 = 5.66 V_2^2 - 5.66 V_2 V_4\cos\left(\delta_2 - \delta_4\right)$$
$$+ 3.33 V_2\sin\left(\delta_2\right) + 30.19 V_2 V_4\sin\left(\delta_2 - \delta_4\right),$$

$$P_3^G = 1.41 V_3^2 - 1.07 V_3\cos\left(\delta_3\right)$$
$$+ \left(-0.29\cos\varphi_{34} - 3.82\sin\varphi_{34}\right) V_3 V_4\cos\left(\delta_3 - \delta_4\right)$$
$$+ 6.73 V_3\sin\left(\delta_3\right) + \left(3.82\cos\varphi_{34} - 0.29\sin\varphi_{34}\right)$$
$$\times V_3 V_4\sin\left(\delta_3 - \delta_4\right)$$
$$+ \frac{3.13}{T_{35}} V_3 V_5\sin\left(\delta_3 - \delta_5\right),$$

$$P_4^G - 0.900 = 5.95 V_4^2 - 5.66 V_4 V_2\cos\left(\delta_4 - \delta_2\right)$$
$$+ \left(-0.29\cos\varphi_{34} + 3.82\sin\varphi_{34}\right) V_4 V_3\cos\left(\delta_4 - \delta_3\right)$$
$$+ 30.19 V_4 V_2\sin\left(\delta_4 - \delta_2\right)$$
$$+ \left(3.82\cos\varphi_{34} + 0.29\sin\varphi_{34}\right) V_4 V_3\sin\left(\delta_4 - \delta_3\right)$$
$$+ 2.00 V_4 V_5\sin\left(\delta_4 - \delta_5\right),$$

$$-0.239 = \frac{3.13}{T_{35}} V_5 V_3\sin\left(\delta_5 - \delta_3\right) + 2.00 V_5 V_4\sin\left(\delta_5 - \delta_4\right),$$

$$Q_1^G = 10.04 - 1.07 V_3\sin\left(-\delta_3\right) - 3.33 V_2\cos\left(-\delta_2\right)$$
$$- 6.73 V_3\cos\left(-\delta_3\right),$$

$$0 = -5.66 V_2 V_4\sin\left(\delta_2 - \delta_4\right) + 33.22 V_2^2$$
$$- 3.33 V_2\cos\left(\delta_2\right) - 30.19 V_2 V_4\cos\left(\delta_2 - \delta_4\right),$$

$$Q_3^G = -1.07 V_3\sin\left(\delta_3\right) + \left(-0.29\cos\varphi_{34} - 3.82\sin\varphi_{34}\right)$$
$$\times V_3 V_4\sin\left(\delta_3 - \delta_4\right)$$
$$+ \left(10.53 + \frac{3.13}{T_{35}^2}\right) V_3^2 - 6.73 V_3\cos\left(\delta_3\right)$$
$$- \left(3.82\cos\varphi_{34} - 0.29\sin\varphi_{34}\right) V_3 V_4\cos\left(\delta_3 - \delta_4\right)$$
$$- \frac{3.13}{T_{35}} V_3 V_5\cos\left(\delta_3 - \delta_5\right),$$

$$Q_4^G - 0.940 = -5.66 V_4 V_2\sin\left(\delta_4 - \delta_2\right)$$
$$+ \left(-0.29\cos\varphi_{34} + 3.82\sin\varphi_{34}\right) V_4 V_3\sin\left(\delta_4 - \delta_3\right)$$
$$+ 36.01 V_4^2 - 30.19 V_4 V_2\cos\left(\delta_4 - \delta_2\right)$$
$$- \left(3.82\cos\varphi_{34} + 0.29\sin\varphi_{34}\right) V_4 V_3\cos\left(\delta_4 - \delta_3\right)$$
$$- 2.00 V_4 V_5\cos\left(\delta_4 - \delta_5\right),$$

$$-0.129 = 5.13 V_5^2 - \frac{3.13}{T_{35}} V_5 V_3\cos\left(\delta_5 - \delta_3\right)$$
$$- 2.00 V_5 V_4\cos\left(\delta_5 - \delta_4\right),$$

$$0.10 \leq P_3^G \leq 0.40,$$
$$0.05 \leq P_4^G \leq 0.40,$$
$$-0.20 \leq Q_3^G \leq 0.30,$$
$$-0.20 \leq Q_4^G \leq 0.20,$$

$$-30.0° \leq \varphi_{34} \leq 30.0°,$$
$$0.95 \leq T_{35} \leq 1.05,$$
$$0.95 \leq V_i \leq 1.05, \quad i \in \{2, 3, 4, 5\},$$
$$-180.0° \leq \delta_i \leq 180.0°, \quad i \in \{2, 3, 4, 5\},$$
$$P_1^G, Q_1^G \text{ unrestricted.}$$

Voltage angles δ_1, δ_2, δ_3, and δ_4 are restricted to one full sweep of the unit circle. Slack bus generator powers P_1^G and Q_1^G are unrestricted, and branch current limits are neglected.

For this formulation, the vector of control variables is

$$u = \left(P_1^G, P_3^G, P_4^G, Q_1^G, Q_3^G, Q_4^G, \varphi_{34}, T_{35} \right)$$

and the vector of state variables is

$$x = (\delta_2, \delta_3, \delta_4, \delta_5, V_2, V_3, V_4, V_5).$$

The optimal solution for this formulation is

$$V_2 \approx 0.981, \quad V_3 \approx 0.957, \quad V_4 \approx 0.968, \quad V_5 \approx 0.959,$$
$$\delta_2 \approx -12.59°, \quad \delta_3 \approx -1.67°, \quad \delta_4 \approx -13.86°, \quad \delta_5 \approx -9.13°,$$
$$P_1^G \approx 0.947, \quad P_3^G \approx 0.192, \quad P_4^G \approx 0.053,$$
$$Q_1^G \approx 0.387, \quad Q_3^G \approx -0.127, \quad Q_4^G \approx 0.200,$$
$$\varphi_{34} \approx 12.38°, \quad T_{35} \approx 0.95,$$

with objective function value 0.4016596. If the controllable phase-shifting and tap-changing transformers are instead fixed to $\varphi_{34} = -3.0°$ and $T_{35} = 0.98$, as originally specified, the optimal solution becomes

$$V_2 \approx 0.983, \quad V_3 \approx 0.964, \quad V_4 \approx 0.970, \quad V_5 \approx 0.950,$$
$$\delta_2 \approx -7.50°, \quad \delta_3 \approx -4.22°, \quad \delta_4 \approx -8.20°, \quad \delta_5 \approx -8.64°,$$
$$P_1^G \approx 0.946, \quad P_3^G \approx 0.195, \quad P_4^G \approx 0.058,$$
$$Q_1^G \approx 0.249, \quad Q_3^G \approx -0.072, \quad Q_4^G \approx 0.200,$$

with objective function value 0.4041438, a cost increase of approximately 0.6%.

As an illustration, we implemented three versions of the classic formulation (5)–(11), augmented with constraints (75) and (76), in the GAMS modeling language. The three versions each use a different form of the power flow equations: (i) polar voltage coordinates with rectangular admittance coordinates (57)–(58), (ii) polar voltage coordinates with polar admittance coordinates (59)–(60), and (iii) rectangular voltage coordinates with rectangular admittance coordinates (61)–(62). The model is publicly available in the publisher's online edition of *IIE Transactions*. For the example, the model yielded identical optimal solutions using three local nonlinear solvers, SNOPT, MINOS, and CONOPT, and verified as globally optimal using the global solver LINDOGlobal.

8. Conclusion

In this article, we have addressed the modeling of power systems, the OPF formulation and common variants, and both theoretical and practical aspects of OPF problems. For the reader interested in learning more, particularly regarding optimization algorithms that have been used for OPF, we recommend any or all of the following.

1. Read the classic papers on OPF (for instance, Dommel and Tinney (1968); Alsac and Stott (1974); Stott and Hobson (1978); Sun *et al.* (1984)). These papers provide a detailed discussion of the foundations of OPF and provide context for more recent work.
2. Review textbooks which describe the OPF problem (Wood and Wollenberg, 1996; Zhu, 2009). These textbooks provide clear, detailed formulations and also provide lists of relevant references, although they often omit foundational material on power system modeling.
3. Review the survey papers on OPF from the past several decades (for instance, Huneault and Galiana (1991); Momoh *et al.* (1999a, 1999b); Frank *et al.* (2012a, 2012b)). Reading the older surveys prior to the more recent ones provides insight into how OPF has developed over time.
4. Experiment with the GAMS OPF formulations provided to accompany Section 7, which are available in the online appendix of *IIE Transactions*. Alternatively, install and experiment with the OPF capabilities available in MATPOWER (Zimmerman *et al.*, 2011). Experimentation with either software will provide insight into the practical challenges of OPF.

The material presented in this article should provide a sufficient foundation for understanding the content of the references cited above and elsewhere in the article.

In recent years, OPF has become one of the most widely researched topics in electric power systems engineering. We hope that this article encourages a similar level of engagement within the operations research community, particularly in the development of new, efficient OPF algorithms.

Notes on contributors

Stephen Frank is a research engineer at the National Renewable Energy Laboratory in Golden, Colorado. Steve obtained a Ph.D. in Electrical Engineering from Colorado School of Mines in 2013. His areas of expertise include electric power distribution systems, DC power systems, linear and nonlinear optimization, and energy informatics. Steve's recent research includes optimal design of microgrids and mixed AC–DC electricity distribution systems, analysis of whole-building DC electricity distribution efficiency, and fault detection and diagnostics algorithms for commercial buildings.

Steffen Rebennack is an Associate Professor in the Division of Economics and Business at the Colorado School of Mines. He obtained his Ph.D. degree in 2010 from the University of Florida. He received an honorable mention for the INFORMS 2010 George B. Dantzig Dissertation Award, the OR Dissertation Award 2011 from the German Operations Research Society, and the ENRE Young Researcher Prize of 2015. His research interests are in dimension-reduction techniques for large-scale optimization problems, particularly in stochastic optimization and global optimization. He applies

his research to real-world optimization problems with a focus on power systems applications.

References

Acha, E., Ambriz-Perez, H. and Fuerte-Esquivel, C.R. (2000) Advanced transformer control modeling in an optimal power flow using Newton's method. *IEEE Transactions on Power Systems*, **15**, 290–298.

Adibi, M.M., Polyak, R.A., Griva, I.A., Mili, L. and Ammari, S. (2003) Optimal transformer tap selection using modified barrier-augmented lagrangian method. *IEEE Transactions on Power Systems*, **18**, 251–257.

Almeida, K.C. and Galiana, F.D. (1996) Critical cases in the optimal power flow. *IEEE Transactions on Power Systems*, **11**, 1509–1518.

Alsac, O., Bright, J., Praise, M. and Stott, B. (1990) Further developments in LP-based optimal power flow. *IEEE Transactions on Power Systems*, **5**, 697–711.

Alsac, O. and Stott, B. (1974) Optimal load flow with steady-state security. *IEEE Transactions on Power Apparatus and Systems*, **93**, 745–751.

Azevedo, A.T., Oliveira, A.L., Rider, M.J. and Soares, S. (2010) How to efficiently incorporate FACTS devices in optimal active power flow model. *Journal of Industrial and Management Optimization*, **6**, 315–331.

Bai, X. and Wei, H. (2009) Semi-definite programming-based method for security-constrained unit commitment with operational and optimal power flow constraints. *IET Generation, Transmission & Distribution*, **3**, 182–197.

Baran, M.E. and Wu, F.F. (1989a) Optimal capacitor placement on radial distribution systems. *IEEE Transactions on Power Delivery*, **4**, 725–734.

Baran, M.E. and Wu, F.F. (1989b) Optimal sizing of capacitors placed on a radial distribution system. *IEEE Transactions on Power Delivery*, **4**, 735–743.

Bertsimas, D., Brown, D.B. and Caramanis, C. (2011) Theory and applications of robust optimization. *SIAM Review*, **53**, 464–501.

Bienstock, D. (2013) Progress on solving power flow problems. *OPTIMA*, **93**, 1–7.

Burchett, R.C., Happ, H.H. and Wirgau, K.A. (1982) Large scale optimal power flow. *IEEE Transactions on Power Apparatus and Systems*, **101**, 3722–3732.

Capitanescu, F. and Wehenkel, L. (2010) Sensitivity-based approaches for handling discrete variables in optimal power flow computations. *IEEE Transactions on Power Systems*, **25**, 1780–1789.

Carpentier, J. (1962) Contribution to the economic dispatch problem. *Bulletin de la Société Française des Electriciens*, **8**, 431–447.

Contaxis, G.C., Delkis, C. and Korres, G. (1986) Decoupled optimal load flow using linear or quadratic programming. *IEEE Transactions on Power Systems*, **I**, 1–7.

Cvijić, S., Feldmann, P. and Ilić, M. (2012) Applications of homotopy for solving AC power flow and AC optimal power flow, in *2012 IEEE Power and Energy Society General Meeting*, IEEE Press, Piscataway, NJ, pp. 1–8.

Dommel, H.W. and Tinney, W.F. (1968) Optimal power flow solutions. *IEEE Transactions on Power Apparatus and Systems*, **87**, 1866–1876.

Farivar, M. and Low, S.H. (2013a) Branch flow model: Relaxations and convexification—Part I. *IEEE Transactions on Power Systems*, **28**, 2554–2564.

Farivar, M. and Low, S.H. (2013b) Branch flow model: Relaxations and convexification—part II. *IEEE Transactions on Power Systems*, **28**, 2565–2572.

Frank, S.M. and Rebennack, S. (2015) Optimal design of mixed AC-DC distribution systems for commercial buildings: A nonconvex generalized Benders decomposition approach. *European Journal of Operational Research*, **242**, 710–729.

Frank, S., Steponavice, I. and Rebennack, S. (2012a) Optimal power flow: A bibliographic survey I, formulations and deterministic methods. *Energy Systems*, **3**, 221–258.

Frank, S., Steponavice, I. and Rebennack, S. (2012b) Optimal power flow: A bibliographic survey II, non-deterministic and hybrid methods. *Energy Systems*, **3**, 259–289.

Freitag, E. and Busam, R. (2009) *Complex Analysis*, Springer, Berlin, Germany.

Glover, J.D., Sarma, M.S. and Overbye, T.J. (2008) *Power System Analysis and Design*, Cengage Learning, Stamford, CT.

Granville, S. (1994) Optimal reactive dispatch through interior point method. *IEEE Transactions on Power Systems*, **9**, 136–146.

Greenberg, M. (1998) *Advanced Engineering Mathematics*, Prentice Hall, Upper Saddle River, NJ.

Han, S.P. (1977) A globally convergent method for nonlinear programming. *Journal of Optimization Theory and Applications*, **22**, 297–309.

Huneault, M. and Galiana, F.D. (1991) A survey of the optimal power flow literature. *IEEE Transactions on Power Systems*, **6**, 762–770.

Lavaei, J. and Low, S.H. (2012) Zero duality gap in optimal power flow problem. *IEEE Transactions on Power Systems*, **27**, 92–107.

Lehmköster, C. (2002) Security constrained optimal power flow for an economical operation of FACTS—Devices in liberalized energy markets. *IEEE Transactions on Power Delivery*, **17**, 603–608.

Low, S.H. (2013) Convex relaxation of optimal power flow: A tutorial, in *Proceedings of Bulk Power System Dynamics and Control—IX Optimization, Security and Control of the Emerging Power Grid*, Rethymnon, Greece, pp. 1–15.

Low, S.H. (2014) Convex relaxation of optimal power flow part I: Formulations and equivalence. *IEEE Transactions on Control of Network Systems*, **1**, 15–27.

Momoh, J.A., El-Hawary, M.E. and Adapa, R. (1999) A review of selected optimal power flow literature to 1993 part I: Nonlinear and quadratic programming approaches. *IEEE Transactions on Power Systems*, **14**, 105–111.

Momoh, J.A., El-Hawary, M.E. and Adapa, R. (1999b) A review of selected optimal power flow literature to 1993 part II: Newton, linear programming and interior point methods. *IEEE Transactions on Power Systems*, **14**, 96–104.

Momoh, J.A., Koessler, R.J., Bond, M.S., Sun, D., Papalexopoulos, A. and Ristanovic, P. (1997) Challenges to optimal power flow. *IEEE Transactions on Power Systems*, **12**, 444–447.

Momoh, J.A., Zhu, J.Z., Boswell, G.D. and Hoffman, S. (2001) Power system security enhancement by OPF with phase shifter. *IEEE Transactions on Power Systems*, **16**, 287–293.

Nocedal, J. and Wright, S. (2006) *Numerical Optimization*, Springer, New York, NY.

O'Malley, J. (2011) *Schaum's Outline of Basic Circuit Analysis*, McGraw-Hill, New York, NY.

Pajic, S. and Clements, K.A. (2005) Power system state estimation via globally convergent methods. *IEEE Transactions on Power Systems*, **20**, 1683–1689.

Peschon, J., Bree, D.W. and Hajdu, L.P. (1972) Optimal power-flow solutions for power system planning. *Proceedings of the IEEE*, **6**, 64–70.

Qiu, W., Flueck, A.J. and Tu, F. (2005) A new parallel algorithm for security constrained optimal power flow with a nonlinear interior point method, in *IEEE Power Engineering Society General Meeting*, IEEE Press, Piscataway, NJ, pp. 2422–2428.

Rardin, R.L. (1997) *Optimization in Operations Research*, Prentice Hall, Upper Saddle River, NJ.

Rau, N.S. (2003a) Issues in the path toward an RTO and standard markets. *IEEE Transactions on Power Systems*, **18**, 435–443.

Rau, N.S. (2003b) *Optimization Principles: Practical Applications to the Operation and Markets of the Electric Power Industry*, Wiley-IEEE Press, Hoboken, NJ.

Snyder, L. (2013) Multi-period optimal power flow problems. *OPTIMA*, **93**, 8–9.

Soler, E.M., de Sousa, V.A. and da Costa, G.M. (2012) A modified primal-dual logarithmic-barrier method for solving the optimal power flow problem with discrete and continuous control variables. *European Journal of Operational Research*, **222**, 616–622.

Sousa, A.A., Torres, G.L. and Canizares, C.A. (2011) Robust optimal power flow solution using trust region and interior-point methods. *IEEE Transactions on Power Systems*, **26**, 487–499.

Stott, B. and Hobson, E. (1978) Power system security control calculation using linear programming parts I and II. *IEEE Transactions on Power Apparatus and Systems*, **97**, 1713–1731.

Stott, B., Jardim, J. and Alsac, O. (2009) DC power flow revisited. *IEEE Transactions on Power Systems*, **24**, 1290–1300.

Sun, D.I., Ashley, B., Brewer, B., Hughes, A. and Tinney, W.F. (1984) Optimal power flow by Newton approach. *IEEE Transactions on Power Apparatus and Systems*, **103**, 2864–2880.

Torres, G.L. and Quintana, V.H. (1998) An interior-point method for nonlinear optimal power flow using voltage rectangular coordinates. *IEEE Transactions on Power Systems*, **13**, 1211–1218.

Vargas, L.S., Quintana, V.H. and Vannelli, A. (1993) A tutorial description of an interior point method and its applications to security-constrained economic dispatch. *IEEE Transactions on Power Systems*, **8**, 1315–1323.

Wang, H., Murillo-Sánchez, C.E., Zimmerman, R.D. and Thomas, R.J. (2007) On computational issues of market-based optimal power flow. *IEEE Transactions on Power Systems*, **22**, 1185–1193.

Wood, A.J. and Wollenberg, B.F. (1996) *Power Generation, Operation, and Control*, John Wiley & Sons, Inc., New York, NY.

Working Group on a Common Format for Exchange of Solved Load Flow Data., (1973) Common format for exchange of solved load flow data. *IEEE Transactions on Power Apparatus and Systems*, **92**, 1916–1925.

Xiao, Y., Song, Y.H. and Sun, Y.-Z. (2002) Power flow control approach to power systems with embedded FACTS devices. *IEEE Transactions on Power Systems*, **17**, 943–950.

Zhang, W., Li, F. and Tolbert, L.M. (2007) Review of reactive power planning: Objectives, constraints, and algorithms. *IEEE Transactions on Power Systems*, **22**, 2177–2186.

Zhang, W. and Tolbert, L.M. (2005) Survey of reactive power planning methods, in *Proceedings of the IEEE Power Engineering Society General Meeting,* vol. 2, IEEE Press, Piscataway, NJ, pp. 1430–1440.

Zhang, X.-P. (2010) *Fundamentals of Electric Power Systems*, John Wiley & Sons, Inc., New York, pp. 1–52.

Zhu, J. (2009) *Optimization of Power System Operation*, Wiley-IEEE, Piscataway, NJ.

Zimmerman, R.D. and Murillo-Sánchez, C.E. (2011) *MATPOWER 4.1 User's Manual*, Power Systems Engineering Research Center, Tempe, Arizona.

Zimmerman, R.D., Murillo-Sánchez, C.E. and Thomas, R.J. (2011) MATPOWER: Steady-state operations, planning, and analysis tools for power systems research and education. *IEEE Transactions on Power Systems*, **26**, 12–19.

Appendices

Appendix A: Notation

This Appendix documents the definitions for the mathematical symbols used throughout the article. See also Section 2.1 for general comments on notation.

A.1. Sets, indices, and dimensions

The following dimensions and indices are used in the OPF formulations within this article:

- N total number of system buses (nodes);
- L total number of system branches (arcs);
- M number of system load (PQ) buses;
- i, k indices corresponding to system buses and branches;
- c contingency case index;
- t time period index.

System branches are indexed as arcs between buses. For example, the branch between buses i and k is denoted by (i, k) or ik.

There is no standard set notation within the OPF literature. (Many authors do not use sets in their formulations.) For convenience, however, we adopt the following sets in this article:

- **N**   set of system buses (nodes);
- **L**   set of system branches (arcs);
- **M**   set of load (PQ) buses;
- **G**   set of controllable generation buses;

- **H**   set of branches with controllable phase-shifting transformers;
- **K**   set of branches with controllable tap-changing transformers;
- **Q**   set of planned locations (buses) for new reactive power sources;
- **C**   set of power system contingencies for contingency analysis;
- **T**   set of time periods for multi-period OPF.

Remarks:

1. We use L to indicate the number of system branches because B is reserved for the bus susceptance matrix.

2. In the optimization community, c often refers to a vector of objective function coefficients. In this article, however, we use uppercase C for objective function coefficients and reserve lowercase c for the contingency case index of SCED described in Section 3.1.

3. For clarity, we use **H** and **K** to represent sets of controllable phase-shifting and tap-changing transformers rather than **S** (often used to designate sources or scenarios) and **T** (often used to designate time periods). The letters H and K otherwise have no special association with phase-shifting and tap-changing transformers.

A.2. Units

The following electrical units are used in this article:

- V   Volt (unit of electrical voltage);
- A   Ampere (unit of electrical current);
- W   Watt (unit of real electrical power);
- VA   Volt-Ampere (unit of apparent electrical power);
- VAR   Volt-Ampere Reactive (unit of reactive electrical power).

Watts, Volt-Amperes, and Volt-Amperes Reactive have the same SI (Système International, that is, metric) unit representation (one Volt times one Ampere) but differ in physical interpretation as described in Appendix B.4.

A.3. Electrical quantities

In power systems analysis, electrical quantities are represented in the frequency domain as phasor quantities (complex numbers). Complex numbers may be represented as a single complex variable, as two real-valued variables in rectangular form $a + jb$, or as two real-valued variables in polar form $c\angle\gamma$; all of these notations are found in the OPF literature. (Complex number notation is explained in more detail in Section B.3.) Here, we document the usual symbols and relationships used for the electrical quantities; some notational exceptions exist in the literature.

A.3.1. Impedance and admittance

- $\widetilde{Z}_{ik}$ complex impedance of branch ik;
- R_{ik} resistance of branch ik (real part of $\widetilde{Z}_{ik}$);
- X_{ik} reactance of branch ik (imaginary part of $\widetilde{Z}_{ik}$) $\widetilde{Z}_{ik} = R_{ik} + jX_{ik}$;
- $\widetilde{y}_{ik}$ complex series admittance of branch ik;
- g_{ik} series conductance of branch ik (real part of $\widetilde{y}_{ik}$);

b_{ik} series susceptance of branch ik (imaginary part of $\widetilde{y}_{ik}$)
$\widetilde{y}_{ik} = 1/\widetilde{Z}_{ik} = g_{ik} + jb_{ik}$;

$\widetilde{y}_i^{\mathrm{S}}$ complex shunt admittance at bus i;

g_i^{S} shunt conductance of bus i (real part of $\widetilde{y}_i^{\mathrm{S}}$);

b_i^{S} shunt susceptance of bus i (imaginary part of $\widetilde{y}_i^{\mathrm{S}}$)
$\widetilde{y}_i^{\mathrm{S}} = g_i^{\mathrm{S}} + jb_i^{\mathrm{S}}$;

$\widetilde{y}_{ik}^{\mathrm{Sh}}$ complex shunt admittance of branch ik;

g_{ik}^{Sh} shunt conductance of branch ik (real part of $\widetilde{y}_{ik}^{\mathrm{Sh}}$);

b_{ik}^{Sh} shunt susceptance of branch ik (imaginary part of $\widetilde{y}_{ik}^{\mathrm{Sh}}$)
$\widetilde{y}_{ik}^{\mathrm{Sh}} = g_{ik}^{\mathrm{Sh}} + jb_{ik}^{\mathrm{Sh}}$;

$\widetilde{Y}_{ik}$ complex ikth element of the bus admittance matrix;

Y_{ik} magnitude of ikth element of the bus admittance matrix;

θ_{ik} angle of ikth element of the bus admittance matrix;

G_{ik} conductance of ikth element of the bus admittance matrix (real part of $\widetilde{Y}_{ik}$);

B_{ik} susceptance of ikth element of the bus admittance matrix (imaginary part of $\widetilde{Y}_{ik}$)
$\widetilde{Y}_{ik} = Y_{ik}\angle\theta_{ik} = G_{ik} + jB_{ik}$.

Note the distinction between lowercase $y, g,$ and b and uppercase $Y, G,$ and B: the former represents the values corresponding to individual system branch elements, whereas the latter refers to the admittance matrix that models the interaction of all system branches.

A.3.2. Voltage

$\widetilde{V}_i$ complex (phasor) voltage at bus i;

V_i voltage magnitude at bus i;

δ_i voltage angle at bus i;

E_i real part of complex voltage at bus i;

F_i imaginary part of complex voltage at bus i $\widetilde{V}_i = V_i\angle\delta_i = E_i + jF_i$.

A.3.3. Current

$\widetilde{I}_i$ complex (phasor) current injected at bus i;

I_i magnitude of current injected at bus i;

$\widetilde{I}_{ik}$ complex (phasor) current in branch ik, directed from bus i to bus k;

I_{ik} magnitude of current in branch ik.

A.3.4. Power

P_i^{L} load (demand) real power at bus i;

Q_i^{L} load (demand) reactive power at bus i;

S_i^{L} load (demand) complex power at bus i $S_i^{\mathrm{L}} = P_i^{\mathrm{L}} + jQ_i^{\mathrm{L}}$;

P_i^{G} generator (supply) real power at bus i;

Q_i^{G} generator (supply) reactive power at bus i;

S_i^{G} generator (supply) complex power at bus i $S_i^{\mathrm{G}} = P_i^{\mathrm{G}} + jQ_i^{\mathrm{G}}$;

P_i net real power injection at bus i ($P_i = P_i^{\mathrm{G}} - P_i^{\mathrm{L}}$);

Q_i net reactive power injection at bus i ($Q_i = Q_i^{\mathrm{G}} - Q_i^{\mathrm{L}}$);

S_i net complex power injection at bus i $S_i = S_i^{\mathrm{G}} - S_i^{\mathrm{L}} = P_i + jQ_i$.

A.3.5. Other

φ_{ik} phase shift of phase-shifting transformer in branch ik;

T_{ik} tap ratio of tap-changing transformer in branch ik.

A.3.6. Comments

The phasor indicator $\widetilde{}$ is omitted for complex power S, as S is always understood to be a complex quantity. In the literature, the indicator $\widetilde{}$ is also often omitted for V, I, y, and Y, but we include it here to disambiguate the complex quantities from their associated (real-valued) magnitudes.

Appendix B: Fundamental concepts

This Appendix summarizes several fundamental concepts of electrical circuit theory and power systems analysis. For further background, we refer interested readers to the excellent textbooks by O'Malley (2011) and Glover *et al.* (2008).

The fundamental electrical quantities are *voltage* and *current*. Voltage describes the potential energy per unit of charge between two nodes in an electric circuit, whereas current describes the flow rate of electric charge between circuit nodes. Voltage and current are analogous to pressure and fluid flow in a hydraulic system. Voltage multiplied by current yields power, that is, energy transfer per unit time.

B.1. Ohm's law

Ohm's law describes the relationship between the voltage V across and the current I flowing through an electrical circuit element, such as a transmission line. Ohm's law states that

$$V = IR,$$

in which resistance R provides the constant of proportionality between voltage and current. Ohm's law as written here applies to direct current (DC) circuits but is readily extended to the steady-state analysis of alternating current (AC) circuits (see Appendix B.3).

B.2. Kirchoff's laws

Electrical circuits consist of nodes (physical points of interconnection) connected by circuit elements, which provide paths for electrical current. Kirchoff's laws govern the physical behavior of electric circuits. KVL states that the sum of voltages around a closed loop in an electrical circuit is equal to zero (Fig. A1(a)). To apply KVL properly, the sign convention for each voltage
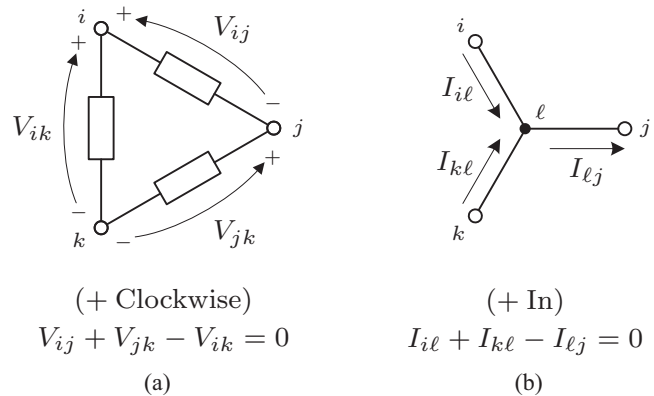

(+ Clockwise)   (+ In)

$V_{ij} + V_{jk} - V_{ik} = 0$ $I_{i\ell} + I_{k\ell} - I_{\ell j} = 0$

(a)   (b)

Figure A1. Illustration of Kirchoff's laws: (a) KVL and (b) KCL.

must be considered: if the positive node for the defined voltage is encountered first while traversing the loop, then the voltage is added; if the negative node is encountered first, then the voltage is subtracted (that is, its inverse is added).

KCL states that the sum of currents at an electrical node is equal to zero (Fig. A1(b)). As with KVL, sign convention is important. Typically, currents defined as entering the node are added, whereas those defined as leaving the node are subtracted. Therefore, KCL may be stated equivalently as follows: the sum of currents entering an electrical node is exactly equal to the sum of currents leaving that node. KCL is the circuit analysis equivalent of flow balance in network theory.

KVL and KCL are complementary; both must be satisfied in any valid solution to a power flow problem. In OPF, KVL and KCL are not enforced directly, but the construction of the admittance matrix ensures that they remain satisfied (see Section 4).

B.3. AC circuit analysis

For power flow analysis, AC electric power systems are analyzed under the assumption of sinusoidal steady-state operation. At sinusoidal steady state, all system voltages and currents are sinusoids with fixed magnitude, frequency, and phase shift. Under these conditions, the time-domain differential equations governing system voltage and current may be transformed into a set of complex algebraic equations in the frequency domain. This *phasor* representation of the system is much easier to solve.

A phasor represents a sinusoidal time-domain signal as a complex exponential in the frequency domain using the relationship

$$\underset{\textit{Time Domain}}{c \sin\left(2\pi f t + \gamma\right)} \quad \Leftrightarrow \quad \underset{\textit{Frequency Domain}}{c e^{j\gamma}}.$$

The frequency f of the signal is fixed and therefore omitted from the phasor notation. The phasor $ce^{j\gamma}$ may be written as $c\angle\gamma$ in polar coordinates or as $a + jb$ in rectangular coordinates, in which, according to Euler's formula,

$$a = c \cos\gamma,$$
$$b = c \sin\gamma,$$
$$c = \sqrt{a^2 + b^2},$$
$$\gamma = \arctan\frac{b}{a}.$$

For voltages and currents, c and γ represent magnitude and phase angle, written as $\widetilde{V} = V\angle\delta$ for voltages and $\widetilde{I} = I\angle\theta$ for currents. In electrical engineering, voltage and current phasors are expressed as Root-Mean-Square (RMS) quantities rather than peak quantities. This is done so that frequency-domain power calculations yield the correct values without the need for a scaling factor. For a sinusoid, the RMS magnitude is $1/\sqrt{2}$ times the peak magnitude. Thus, the time-domain voltage waveform

$$V_{\text{Pk}} \sin\left(2\pi f t + \delta\right)$$

has the frequency domain phasor

$$\frac{V_{\text{Pk}}}{\sqrt{2}} e^{j\delta}.$$

Ohm's law, KVL, and KCL remain valid for AC circuit analysis. For AC quantities, Ohm's law takes the form

$$\widetilde{V} = \widetilde{I}\widetilde{Z},$$

in which $\widetilde{Z} = R + jX$ is the complex *impedance* that describes the relationship between sinusoidal voltage $\widetilde{V}$ and sinusoidal current $\widetilde{I}$ for a particular circuit element. Resistance R models power consumption, and *reactance X* represents the effect of electrical storage (capacitors and inductors). At steady state, storage elements absorb and release energy during different portions of the AC cycle, producing a phase shift between voltage and current. It is also common to write Ohm's law in the form

$$\widetilde{Y}\widetilde{V} = \widetilde{I},$$

in which $\widetilde{Y} = 1/\widetilde{Z}$ is the *admittance*, the reciprocal of impedance. In rectangular coordinates, $\widetilde{Y} = G + jB$, in which G is the *conductance* and B is the *susceptance*.

B.4. Complex power

Power is the rate of energy transfer; that is, the derivative of energy with respect to time. In the time domain, electrical power is the product of voltage and current. In AC power systems, however, instantaneous electrical power fluctuates as voltage and current magnitude and polarity change over time. For frequency-domain analysis, power systems engineers use the concept of *complex power* to characterize these time-domain power fluctuations.

Complex power is a phasor quantity consisting of *real power* and *reactive power*. Real power represents real work, that is, a net transfer of energy from source to load over time. Reactive power, on the other hand, represents circulating energy—a cyclic exchange of energy that averages zero net energy transfer over time. Reactive power is sometimes called *imaginary power*, both because it does not perform real work and because it is the imaginary component of the phasor.

Real power transfer occurs when voltage and current are in phase, whereas reactive power transfer occurs when voltage and current are 90° out of phase (that is, orthogonal). Given a reference voltage $v(t)$, an arbitrary (time domain) AC current $i(t)$ can be represented by the sum of a direct component $i_d(t)$ (in phase with the voltage) and quadrature component $i_q(t)$ (orthogonal to the voltage). The direct component corresponds to real power and the quadrature component reactive power, as illustrated in Fig. A2.

By convention, reactive power is considered positive when current lags voltage. Therefore, complex power S is given by

$$S = \widetilde{V}\widetilde{I}^* = P + jQ$$

and consists of orthogonal components P (real power) and Q (reactive power). (Here and elsewhere in this article, the symbol * denotes complex conjugation rather than an optimal value; this use is typical in electrical engineering.) The magnitude of complex power, $|S|$, is called the *apparent power* and is often used to specify power systems equipment and transmission line ratings. Complex and apparent power have units of Volt-Amperes (VA), real power has units of Watts (W), and reactive power has units of Volt-Amperes Reactive (VAR).
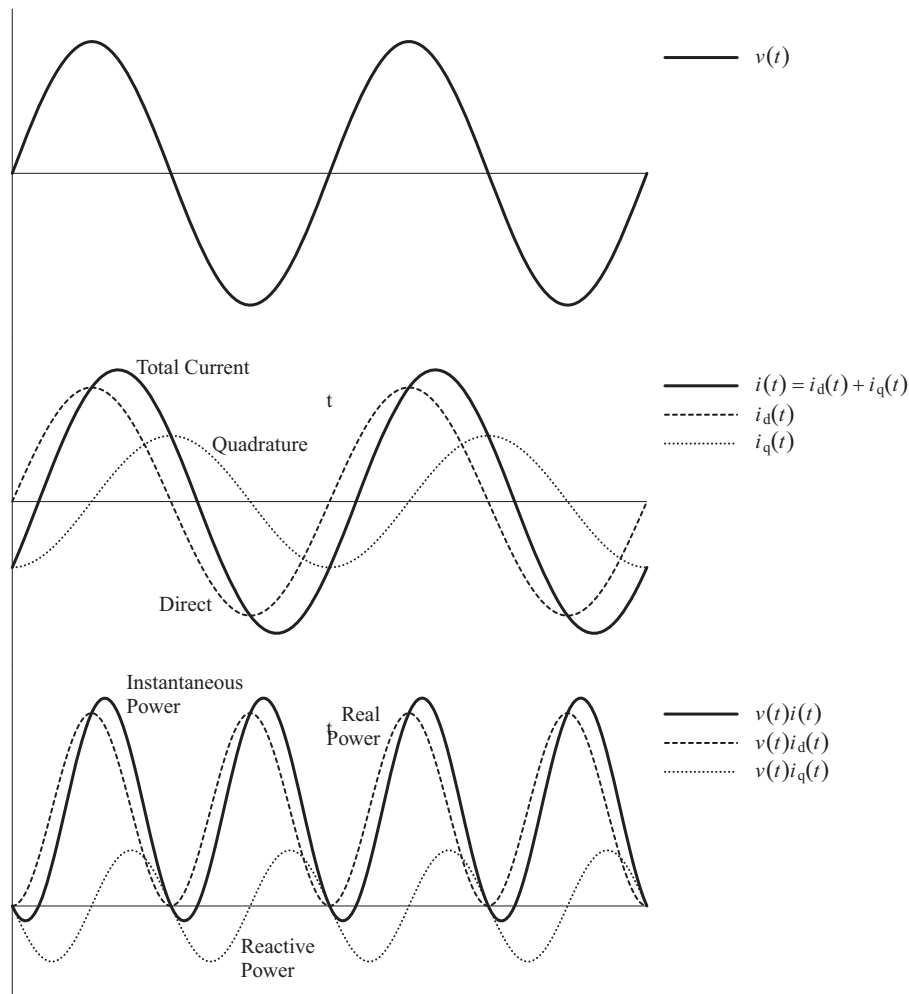
Figure A2. Conceptual illustration of real and reactive power using time-domain waveforms. In the figure, current $i(t)$ lags voltage $v(t)$ by 30°.

Appendix C: The per unit system

In power systems analysis, electrical quantities are usually expressed as a ratio of the actual SI quantity to a reference, or *base*, quantity; this transformation of variables is called the *per unit* system. Base quantities have SI units (Volts, Amperes, Ohms, etc.), and per unit quantities are dimensionless and are labeled using a designation, if any, of "p.u." The per unit value of an SI quantity x on a given base x_{Base} is

$$x_{\text{pu}} = \frac{x}{x_{\text{Base}}}.$$

Correct interpretation of the SI value of a per unit quantity therefore requires knowledge of the base quantity. For example, a power of 0.15 p.u. on a 10 MVA base equals 1.5 MW, but 0.15 p.u. on a 1000 MVA base equals 150 MW. (In per unit, real power, reactive power, and apparent power share a common base with units of VA.)

In power systems analysis, base quantities exist for voltage, current, power, impedance, and admittance. Once any two system bases are specified, the others are fixed exactly. In three-phase PF analysis, convention is to specify the voltage and power bases,

$$V_{\text{Base}} = \text{Line-to-line Voltage},$$

$$S_{\text{Base}} = \text{Three-phase Power},$$

and calculate the remaining system bases according to

$$I_{\text{Base}} = \frac{S_{\text{Base}}}{\sqrt{3}\, V_{\text{Base}}},$$

$$Z_{\text{Base}} = \frac{V_{\text{Base}}}{\sqrt{3}\, I_{\text{Base}}} = \frac{V_{\text{Base}}^2}{S_{\text{Base}}},$$

$$Y_{\text{Base}} = \frac{\sqrt{3}\, I_{\text{Base}}}{V_{\text{Base}}} = \frac{S_{\text{Base}}}{V_{\text{Base}}^2} = \frac{1}{Z_{\text{Base}}}.$$

For mathematical convenience, power systems engineers typically set S_{Base} to one of 10, 100, or 1000 MVA and select V_{Base} as the nominal line-to-line voltage at each bus. Thus, S_{Base} is constant throughout the power system, but the other bases are distinct at each system bus. When V_{Base} is selected in this way, the voltage ratio of most system transformers becomes 1:1 in per unit, simplifying the development of the system admittance matrix (Section 4).

With a proper selection of system bases, the per unit system has several advantages over the SI system of measurement, most notably as follows.

1. Per Unit quantities have consistent magnitudes on the order of 1.0, which improves the numerical stability of power flow calculations.

2. The use of per unit eliminates the need to distinguish between single-phase and three-phase electrical quantities.

3. The use of per unit eliminates the need to apply voltage and current scaling factors at the majority of system transformers.

4. The per unit system is easier to interpret at a glance. (For example, per unit voltage should always lie within the approximate range 0.95–1.05 p.u., regardless of the SI voltage.)

An in-depth discussion of these advantages is beyond the scope of this article; we instead refer the interested reader to Glover *et al.* (2008).

All calculations that can be performed in the SI system can also be performed in per unit. However, (i) per unit and SI quantities cannot be mixed in calculations, and (ii) all per unit calculations must be performed on a consistent set of bases. Power systems texts frequently mix per unit and SI units, for instance, reporting power in MW but voltage in per unit. In OPF, convention is to specify source and load power in SI units, indicate the system power base, and specify all other quantities directly in per unit (see Appendix D). The powers must be converted to per unit prior to evaluating the power flow equations, but no other conversions are usually necessary.

Appendix D: Data exchange

Two common formats for the academic exchange of power flow and OPF case data are the IEEE Common Data Format (Working Group on a Common Format for Exchange of Solved Load Flow Data, 1973) and the MATPOWER Case Format (Zimmerman and Murillo-Sánchez, 2011). Most power systems data are proprietary. However, a few publicly available test cases for OPF are distributed in one or both of these formats (see http://www.ee.washington.edu/research/pstca/ and Zimmerman and Murillo-Sánchez, 2011), and many OPF researchers use these test cases to benchmark algorithms. This section summarizes the structure of these formats and their relationship to the classic OPF formulation; the goal is to assist the reader in interpreting and applying the limited available published data.

D.1. The IEEE common data format

The IEEE Common Data Format (CDF) was first developed in order to standardize the exchange of PF case data among utility companies (Working Group on a Common Format for Exchange of Solved Load Flow Data, 1973). It has since been used to archive and exchange power systems test case data for the purpose of testing conventional PF and OPF algorithms. The format includes sections, or "cards," for title data, bus data, branch data, loss zone data, and interchange data. (Originally, utilities exchanged CDF data by mail on paper card media.) Only the title, bus, and branch data are relevant for classic OPF as described in this article. The full specification for the IEEE CDF can be found in Working Group on a Common Format for Exchange of Solved Load Flow

Table D1. Field specification for IEEE CDF bus data. The sixth column maps the field to an index, parameter, or variable used in the classic OPF formulation given in Section 2.4. (Some fields are used indirectly via inclusion in $\hat{Y}$.)

Field	Columns	Field name	Data type	Units	Quantity in OPF
1	1–4	Bus Number	Integer		i (bus index)
2	6–17	Bus Name	Text		
3	19–20	Bus Area	Integer		
4	21–23	Loss Zone Number[a]	Integer		
5	26	Bus Type	Integer		Special[b]
6	28–33	Voltage Magnitude	Numeric	p.u.	V_i
7	34–40	Voltage Angle	Numeric	deg.	δ_i
8	41–49	Load Real Power	Numeric	MW	P_i^{L}
9	50–58	Load Reactive Power	Numeric	MVAR	Q_i^{L}
10	59–67	Gen. Real Power	Numeric	MW	P_i^{G}
11	68–75	Gen. Reactive Power	Numeric	MVAR	Q_i^{G}
12	77–83	Base Voltage[a]	Numeric	kV	
13	85–90	Desired Voltage	Numeric	p.u.	V_i (Special[c])
14	91–98	Max. Reactive Power	Numeric	MVAR	$Q_i^{\mathrm{G,max}}$
		or			
		Max. Voltage Magnitude[d]	Numeric	p.u.	V_i^{max}
15	99–106	Min. Reactive Power	Numeric	MVAR	$Q_i^{\mathrm{G,min}}$
		or			
		Min. Voltage Magnitude[d]	Numeric	p.u.	V_i^{min}
16	107–114	Bus Shunt Conductance	Numeric	p.u.	g_i^{S}
17	115–122	Bus Shunt Susceptance	Numeric	p.u.	b_i^{S}
18	124–127	Remote Bus Number	Integer		

[a]Optional field.
[b] 0 = PQ, 1 = PQ (within voltage limits), 2 = PV (within VAR limits), 3 = Swing.
[c]Indicates target voltage magnitude for voltage-controlled (PV) buses.
[d]Gives reactive power limits if bus type is 2, voltage limits if bus type is 1.

Data (1973) and an abbreviated description is available at http://www.ee.washington.edu/research/pstca/.

Each IEEE CDF data card consists of plain text with fields delimited by character column. The title data card is a single line that includes summary information for the case, including the power base S_{Base} in MVA. The bus and branch data cards follow, beginning with the characters BUS DATA FOLLOWS and BRANCH DATA FOLLOWS, respectively, and ending with the flag characters -999. Each line within the card gives the data for a single bus or branch.

Tables D1 and D2 list the IEEE CDF field specifications for bus and branch data, respectively. The fields include a mixture of SI and per unit quantities. Conversion of all quantities to per unit is required prior to use in an OPF formulation. Nominal-valued and unused fields in the data have zero entries. This quirk of the specification requires some caution in processing the data; for example, a value of 0.0 in the branch voltage ratio field should be interpreted as a nominal tap ratio ($T = 1.0$).

The IEEE CDF format is adapted to the compact exchange of system control data rather than OPF data. The field structure therefore has several limitations:

1. Some IEEE CDF fields specify final variable values (for instance, voltages V_i) for conventional PF. For OPF, these fields should be understood as a feasible or near-feasible starting point rather than an optimal solution. (Due to rounding, the reported solution may not be strictly feasible.)

Table D2. Field specification for IEEE CDF branch data. The sixth column maps the field to an index, parameter, or variable used in the classical OPF formulation given in Section 2.4. (Some fields are used indirectly via inclusion in $\widetilde{Y}$.)

Field	Columns	Field name	Data type	Units	Quantity in OPF
1	1–4	Tap Bus Number	Integer		i (from bus index)
2	6–9	Z Bus Number	Integer		k (to bus index)
3	11–12	Line Area[a]	Integer		
4	13–15	Loss Zone Number[a]	Integer		
5	17	Circuit Number	Integer		
6	19	Branch Type	Integer		Special[b]
7	20–29	Branch Resistance	Numeric	p.u.	R_{ik}
8	30–39	Branch Reactance	Numeric	p.u.	X_{ik}
9	41–49	Branch Shunt Susceptance	Numeric	p.u.	b_{ik}^{Sh}
10	51–55	Line Rating 1[a,c]	Numeric	MVA	$l_{ik}^{\max}$
11	57–61	Line Rating 2[a]	Numeric	MVA	
12	63–67	Line Rating 3[a]	Numeric	MVA	
13	69–72	Control Bus Number	Integer		
14	74	Side	Integer		
15	77–82	Voltage Ratio	Numeric	p.u.	T_{ik}
16	84–90	Phase Angle	Numeric	deg.	φ_{ik}
17	91–97	Min. Voltage Tap	Numeric	p.u.	$T_{ik}^{\min}$
		or			
		Min. Phase Angle[d]	Numeric	deg.	$\varphi_{ik}^{\min}$
18	98–104	Max. Voltage Tap	Numeric	p.u.	$T_{ik}^{\max}$
		or			
		Max. Phase Angle[d]	Numeric	deg.	$\varphi_{ik}^{\max}$
19	105–111	Tap Step Size	Numeric	p.u.	
		or			
		Phase Angle Step Size[d]	Numeric	deg.	
20	113–119	Min. Voltage	Numeric	p.u.	
		or			
		Min. MVar Transfer	Numeric	MVar	
		or			
		Min. MW Transfer[e]	Numeric	MW	
21	120–126	Max. Voltage	Numeric	p.u.	
		or			
		Max. MVar Transfer	Numeric	MVar	
		or			
		Max. MW Transfer[e]	Numeric	MW	

[a] Optional field.
[b] 0 = Transmission line, 1 = Fixed T and φ, 2 = Controllable T and fixed φ (voltage control), 3 = Controllable T and fixed φ (MVAR control), 4 = Fixed T and controllable φ.
[c] Conversion to per-unit current (using rated branch voltage) is required.
[d] Gives voltage tap limits or step if branch type is 2 or 3, phase angle limits or step if branch type is 4.
[e] Gives voltage limits if branch type is 2, MVAR limits if branch type is 3, MW limits if branch type is 4.

2. The fields bus type (bus field 5) and branch type (branch field 6) specify system control methods and are therefore of limited use in OPF. However, the bus and branch types govern the interpretation of certain other fields in the IEEE CDF, as described in the table footnotes. For example, for PQ buses, bus fields 14 and 15 give voltage limits $V_i^{\max}$ and $V_i^{\min}$, respectively. For PV buses, these same fields instead give reactive power generation limits $Q_i^{\mathrm{G,max}}$ and $Q_i^{\mathrm{G,min}}$, respectively.

3. For IEEE CDF fields that depend on the bus and branch types, the data are sufficient for conventional PF but

Table D3. Field specification for bus data matrix in MATPOWER case data (input fields only). The fifth column maps the field to an index, parameter, or variable used in the classic OPF formulation given in Section 2.4. (Some fields are used indirectly via inclusion in $\widetilde{Y}$.)

Column	Field description	Data type	Units	Quantity in OPF
1	Bus Number	Integer		i (bus index)
2	Bus Type	Integer		Special[a]
3	Load Real Power	Numeric	MW	P_i^{L}
4	Load Reactive Power	Numeric	MVAR	Q_i^{L}
5	Bus Area	Integer		
6	Bus Shunt Conductance	Numeric	MW[b]	g_i^{S}
7	Bus Shunt Susceptance	Numeric	MVAR[b]	b_i^{S}
8	Voltage Magnitude	Numeric	p.u.	V_i
9	Voltage Angle	Numeric	deg.	δ_i
10	Base Voltage	Numeric	kV	
11	Loss Zone	Integer		
12	Max. Voltage Magnitude	Numeric	p.u.	$V_i^{\max}$
13	Min. Voltage Magnitude	Numeric	p.u.	$V_i^{\min}$

[a] 1 = PV, 2 = PQ, 3 = Swing, 4 = Isolated.
[b] Specified as a MW or MVAR demand for V = 1.0 p.u.

incomplete for OPF. For example, the IEEE CDF lacks voltage limits for PV buses and reactive power generation limits at PQ buses; the field structure prevents these data from being available. The user must supply (or assume) values for the incomplete data.

4. The IEEE CDF lacks other data required for OPF, including generator real power limits and cost data.

Given these limitations, publicly archived IEEE CDF case data are most useful for obtaining the network structure and associated bus and branch admittance data.

D.2. MATPOWER case format

MATPOWER (Zimmerman *et al.*, 2011) is an open-source software package for MATLAB that includes functions for both conventional PF and OPF. The MATPOWER case format is a set of standard matrix structures used to store power systems case data and closely resembles the IEEE CDF. MATPOWER case data consists of a MATLAB structure with fields `baseMVA`, `bus`, `branch`, `gen`, and `gencost`. `baseMVA` is a scalar giving the system power base S_{Base} in MVA. The remaining fields are matrices. Like the IEEE CDF, the MATPOWER case structure uses a mixture of SI and per unit quantities and specifies nominal-valued branch tap ratios as 0 instead of 1.0. The format is described in detail in the MATPOWER manual (Zimmerman and Murillo-Sánchez, 2011).

Tables D3, D4, and D5 describe the `bus`, `branch`, and `gen` matrices. The `gencost` matrix has the same number of rows as the `gen` matrix, but the column structure provides a flexible description of the generator cost function. Column 1 specifies the type of cost model: 1 for piecewise linear or 2 for polynomial. Columns 2 and 3 give the generator startup and shutdown costs. The interpretation of column numbers 4 and greater depends on the type of cost model.

- For a piecewise linear cost model, column 4 specifies the number of coordinate pairs n of the form (P, C) that generate the piecewise linear cost function. The next $2n$

Table D4. Field specification for branch data matrix in MATPOWER case data (input fields 1–11 only). The fifth column maps the field to an index, parameter, or variable used in the classic OPF formulation given in Section 2.4. (Some fields are used indirectly via inclusion in $\widetilde{Y}$.)

Column	Field description	Data type	Units	Quantity in OPF
1	Tap Bus Number	Integer		i (from bus index)
2	Z Bus Number	Integer		k (to bus index)
3	Branch Resistance	Numeric	p.u.	R_{ik}
4	Branch Reactance	Numeric	p.u.	X_{ik}
5	Branch Shunt Susceptance	Numeric	p.u.	b_{ik}^{Sh}
6	Line Rating (Long-term)[a]	Numeric	MVA	$I_{ik}^{\max}$
7	Line Rating (Short-term)[a]	Numeric	MVA	
8	Line Rating (Emergency)[a]	Numeric	MVA	
9	Voltage Ratio	Numeric	p.u.	T_{ik}
10	Phase Angle	Numeric	deg.	φ_{ik}
11	Branch Status	Binary		

[a] Conversion to per unit current (using rated branch voltage) is required.

Table D5. Field specification for generator data matrix in MATPOWER case data (input fields 1–10 only). The fifth column maps the field to an index, parameter, or variable used in the classic OPF formulation given in Section 2.4.

Column	Field description	Data type	Units	Quantity in OPF
1	Bus Number	Integer		i (generator index)
2	Gen. Real Power	Numeric	MW	P_i^{G}
3	Gen. Reactive Power	Numeric	MVAR	Q_i^{G}
4	Max. Reactive Power	Numeric	MVAR	$Q_i^{\mathrm{G,max}}$
5	Min. Reactive Power	Numeric	MVAR	$Q_i^{\mathrm{G,min}}$
6	Voltage Setpoint	Numeric	p.u.	
7	Gen. MVA Base[a]	Numeric	MVA	
8	Generator Status[b]	Binary		
9	Max. Real Power	Numeric	MW	$P_i^{\mathrm{G,max}}$
10	Min. Real Power	Numeric	MW	$P_i^{\mathrm{G,min}}$

[a] Defaults to system power base S_{Base}.
[b] 0 indicates generator out of service (remove from OPF formulation).

columns, beginning with column 5, give the coordinate pairs $(P_0, C_0), \ldots, (P_{n-1}, C_{n-1})$, in ascending order. The units of C are \$/h and the units of P are MW.

- For a polynomial cost model, column 4 specifies the number n of polynomial cost coefficients. The next n columns, beginning with column 5, give the cost coefficients $C_{n-1}, \ldots, C_0$ in descending order. The corresponding polynomial cost model is $C_{n-1}P^{n-1} + \cdots + C_1 P + C_0$. The units are such that the cost evaluates to dollars \$/h for power given in MW.

If gencost is included, then MATPOWER case data contain nearly all of the information necessary to formulate the classic OPF problem as described in Section 2.4. However, MATPOWER makes no provision for including transformer tap ratios or phase-shifting transformer angles in the set of decision variables; therefore, limits on these variables are not present in the data structure. The user must supply limits for these controls if they exist in the formulation.